

# Minority Reports: Balancing Cost and Quality in Ground Truth Data Annotation

Hsuan Wei Liao<sup>1</sup>, Christopher Klugmann<sup>2</sup>, Daniel Kondermann<sup>2</sup>, Rafid Mahmood<sup>1,3</sup>

<sup>1</sup>Telfer School of Management, University of Ottawa, {hliao009, rmahmood}@uottawa.ca

<sup>2</sup>Quality Match, {ck, dk}@quality-match.com

<sup>3</sup>NVIDIA

High-quality data annotation is an essential but laborious and costly aspect of developing machine learning-based software. We explore the inherent tradeoff between annotation accuracy and cost by detecting and removing minority reports—instances where annotators provide incorrect responses—that indicate unnecessary redundancy in task assignments. We propose an approach to prune potentially redundant annotation task assignments before they are executed by estimating the likelihood of an annotator disagreeing with the majority vote for a given task. Our approach is informed by an empirical analysis over computer vision datasets annotated by a professional data annotation platform, which reveals that the likelihood of a minority report event is dependent primarily on image ambiguity, worker variability, and worker fatigue. Simulations over these datasets show that we can reduce the number of annotations required by over 60% with a small compromise in label quality, saving approximately 6.6 days-equivalent of labor. Our approach provides annotation service platforms with a method to balance cost and dataset quality. Machine learning practitioners can tailor annotation accuracy levels according to specific application needs, thereby optimizing budget allocation while maintaining the data quality necessary for critical settings like autonomous driving technology.

---

## 1. Introduction

Machine learning (ML) is the fundamental component of most image recognition-based software from video conferencing to robotics and autonomous vehicles. The most critical challenge in developing ML models for these systems is the availability of high-quality *labeled* data to train the models (Dimensional Research 2019). For example, consider the perception technology in autonomous vehicles used to detect obstacles and plan routes. Autonomous vehicle developers collect billions of miles of driving video data per year to improve the underlying models (Bigelow and Brulte 2024), but this data must first be annotated with the location and type of obstacles in every video frame before being used for model development (Braun et al. 2019). Moreover, the annotation process has historically been performed by manual human labor. Given the immense volume of data, annotation grows tremendously expensive.

Data annotation can be performed by teams within the firms developing the ML models or outsourced to annotation platforms (Gonzalez-Cabello et al. 2024). There exist different paradigms on managing annotation depending on the ML problem at hand (Hanbury 2008, Song et al. 2022, Tan et al. 2024). In this work, we analyze computer vision problems that require identifying attributes of objects in images, but remark that our results naturally generalize to other ML tasks. For our setting, annotation involves designing a series of multiple choice or true/false questions or tasks that can be posed for each image or cropped segment of an image in the dataset (e.g., ‘is the object in the image a pedestrian?’). These tasks are assigned—often via randomized matching (Karger et al. 2014)—to a team of human annotators to complete.

Annotation is manual online labor performed over long hours by workers sometimes as their primary income source (Horton and Chilton 2010, Berg et al. 2018). Individual workers may make mistakes in labeling, due to factors such as the complexity or ambiguity of the task (e.g., analyzing objects that are partially occluded in images), variable worker skill levels, and fatigue after working long hours. Given the likelihood for individual errors, each task is repeated by a set of annotators and their responses are aggregated to create accurate ‘ground truth’ labels (Karger et al. 2014, Khetan and Oh 2016, Liao et al. 2021). This repetition multiplies the overall cost of labeling a dataset. Consequently, the firms developing the ML models must balance a tradeoff between label quality and cost, depending on the downstream application and the acceptable error tolerance of the overall software. Even well-known benchmark datasets have erroneous labels for between 1 to 10% of their images; the most famous image classification dataset for example, ImageNet (Deng et al. 2009), is estimated to have errors on 5.8% of their image labels (Northcutt et al. 2021).

In this paper, we explore the tradeoff between annotation costs, measured by the total number of annotation tasks completed, and quality, measured by the proportion of labels that change with more repeated annotations, referred to as repeats. Our approach is premised on the intuitive notion that conditioned ex post on a task with multiple repeats, the workers who had submitted different responses from the aggregated answer are giving unnecessary redundancy for the task. We refer to such responses as *minority reports* that contradict the ground truth annotation. We observe that, given an oracle capable of identifying when an annotator will produce a minority report for an assigned task, we

can instead re-assign the worker to other tasks. In place of this acausal oracle, we predict the likelihood of a minority report for each potential task assignment. We then prune assignments with high predicted probabilities, which incurs some risk of these lower-cost aggregated labels changing from their counterfactual ground truth values.

We develop our framework in collaboration with Quality Match, a high-quality data annotation provider. Given a dataset to label, Quality Match’s in-house service determines an ontology for the dataset, estimates the number of repeated annotations needed for each annotation task, and assigns these tasks to a pool of annotators. Using Quality Match’s service, we annotate two datasets for benchmark computer vision problems with 196,446 and 16,000 annotation tasks, respectively (Braun et al. 2019, Alibeigi et al. 2023). The first dataset is annotated according to Quality Match’s standard operational pipeline where the number of repeats is dynamically determined between five to 12, while the second dataset is annotated by a constant number of 11 workers for each task.

For each computer vision problem, we develop a predictive model to estimate the likelihood of a worker to generate a minority report. Our empirical analysis over both datasets reveals that this likelihood is governed almost entirely via three key factors:

- **Image ambiguity:** Objects that are partially occluded, in the distance, or blurry, are more challenging to annotate. There remains a small subset of images for which the odds of a minority report being generated increase by at least  $20\times$ .
- **Annotator variability:** Worker quality is symmetric with high variance. At worst, certain workers can increase the odds of producing minority reports by up to  $54\times$ .
- **Fatigue:** Workers behave according to a bathtub curve when subject to long continuous working periods. Workers are more likely to produce minority reports at the start (i.e., warm-up) and at the end (i.e., exhaustion) of a shift.

Motivated by these empirical insights, we propose a framework to predict, given an annotation task and worker, the likelihood of yielding a minority report, and prescribe whether to enable this task to be completed or to remove the assignment, thereby reducing the total number of annotations requested. Figure 1 visualizes our framework, which employs a simple model that can be inserted into any existing annotation platform. We theoretically show that pruning task assignments follows a ‘no free lunch’ principle, where for any predictive model, pruning always degrades the quality of the dataset by potentially changing the final aggregated labels from their counterfactual ground truths. Nonetheless,

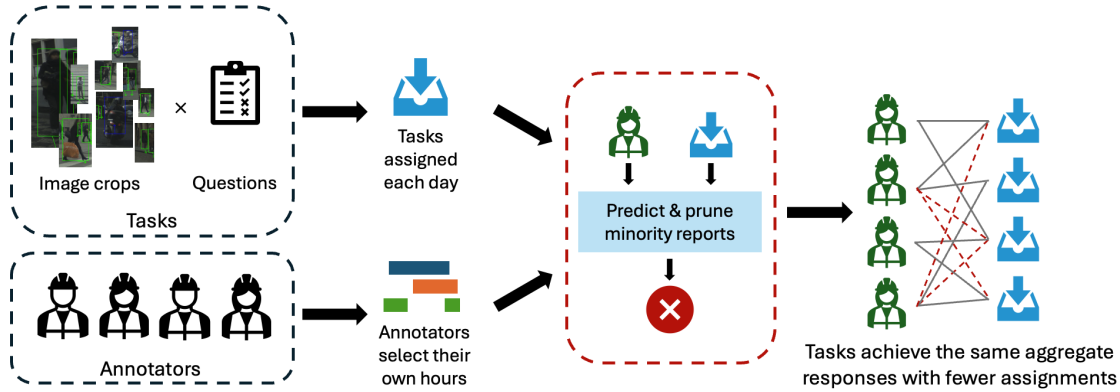


**Figure 1** Overview of our method. Our prescriptive pruning framework can slot into any annotation pipeline after tasks are assigned but before they are executed to reduce costs.

our approach can significantly reduce annotation costs at only a marginal drop in dataset quality. When applied to our datasets, a conservative pruning strategy can prune approximately 22% of the assigned tasks while preserving over 99% of the majority vote labels, and that an aggressive strategy can prune 60% of the assignments while preserving over 96% of the majority votes.

Our contributions are:

1. We analyze factors affecting erroneous annotations in the labeling of ML data to show that image ambiguity, worker skill variability, and worker fatigue capture the likelihood of annotators erring from the majority vote almost completely.
2. We develop a prescriptive framework to forecast in real-time whether an annotator will disagree with the future crowd decision and determine whether to remove task assignments. Simulations show that our strategy can yield up to a 60% decrease in the number of annotations at less than 4% loss in dataset quality.
3. We theoretically analyze this framework to show that while pruning will always lead to a drop in quality, an accurate predictive model can significantly reduce the total number of annotations. This further yields rule-of-thumb guidelines for the average number of repeats needed to annotate a given dataset.

## 2. Related literature

Training ML models requires large data sets that are accurately annotated. Nonetheless, most datasets have some varying noise in their labels (Song et al. 2022, Liao et al. 2024, Durasov et al. 2024). For instance, classic benchmark datasets such as ImageNet (Deng

et al. 2009), were constructed using crowd-sourced annotation efforts, and are known to have errors for approximately 5.8% of the image data points (Northcutt et al. 2021).

ML dataset annotation consists of large operational pipelines that have become key components of enterprise ML engineering teams (Dimensional Research 2019). First, individual tasks for annotating data points are assigned to workers in an online labor pool. While workforce allocation is a well-studied operational problem (see Bouajaja and Dridi (2017) for a review) with applications in assembly lines (Vila and Pereira 2014), crowdsourcing (Wang et al. 2017, Tian et al. 2022, Manshadi and Rodilitz 2022, Fatehi and Wagner 2022), finance (Stratman et al. 2024), and healthcare (Lanzarone and Matta 2014, Adelman et al. 2024), task assignment for data annotation is most commonly achieved via randomized matching (Karger et al. 2014). This requires minimal implementation effort, making it attractive in practice. Once tasks are completed, the labels must be aggregated. The naive approach to creating accurate ‘ground truth’ datasets is by computing a majority vote from a group of workers. More sophisticated techniques determine weighted averages by estimating annotator ability and task difficulty using expectation-maximization (Dawid and Skene 1979, Raykar et al. 2010, Yin et al. 2021, Palley and Satopää 2023), optimization (Karger et al. 2014, Khetan and Oh 2016), dynamic policies (Wang et al. 2017), and end-to-end combined annotation and learning (Rodrigues and Pereira 2018, Tanno et al. 2019, Goh et al. 2023). In contrast to this literature, our prescriptive pruning framework lies in the interim between tasks being assigned but not completed. Given an arbitrary assignment of tasks, we predict which task assignments are likely to be redundant and prune them.

Annotation tasks are relatively low-paying and can be completed quickly, which can lead crowd-sourced workers to be unengaged, make errors, or potentially ‘cheat’ the system, for example by giving random answers (Staats and Gino 2012, Karger et al. 2014). A key challenge remains to identify and prevent such adversarial workers from completing tasks with erroneous labels that poison the aggregated ground truth. Most closely related to our work is by Jagabathula et al. (2017), who propose several algorithms for filtering adversarial workers by penalizing the number of times they have previously disagreed with the majority vote. This filtering can be performed after tasks are completed with the goal of eventually removing adversarial workers from the labor pool. In contrast, we estimate the likelihood of a worker disagreeing with the majority in a future task as a function of

the worker’s latent ‘skill’ level. Rather than removing the worker, our treatment removes task assignments that are predicted to be unfavorable. In the case where workers are of extremely low skill, this may automatically prune all assignments and indirectly remove the worker.

Online labor platforms have enabled on-demand work such as data annotation at massive scales beyond traditional employment structures (Kittur et al. 2013, Horton and Chilton 2010, Horton 2011). This ‘gig’ workforce faces several ongoing frictions including low pay, unstable demand, and constrained task deadlines, in particular for data annotation tasks (Berg et al. 2018, Yin et al. 2018, Gonzalez-Cabello et al. 2024). Managing this workforce raises new questions about engagement and retention to ensure tasks are completed to a high degree of quality. For example, game-theoretic models reveal how optimal fees can balance platform profit with worker participation (Wen and Lin 2016). Moreover, contract design for online crowdwork is a principal agent problem that can be designed with incentives to optimize the quality of completed annotation tasks (Kaynar and Siddiq 2023). Most recently, Liu et al. (2024) explore contract mechanisms for data annotation for large-language models (LLM) in ML. Our work contributes towards quality control in data annotation gig work by simultaneously exploring task difficulty, worker skills, and worker fatigue in an easy-to-learn framework that can derive just-in-time insights before tasks are completed.

Finally, our work is related to the broader empirical literature on worker behavior and productivity. Factors such as task switching (Jin et al. 2020), work interruption (Gurvich et al. 2020, Cai et al. 2018), task specialization (Narayanan et al. 2009, Staats and Gino 2012), and prior experience (Kc and Staats 2012) are known to strongly affect worker productivity in various domains including healthcare, manufacturing, finance, and software development. The labor in our setting consists primarily of low-skill, repetitive tasks that are individually completed within seconds. Our empirical analysis demonstrates that in this online labor setting, variability in the quality of completed tasks depends primarily on individual worker ability, task difficulty, and worker fatigue, in order of importance.

### **3. Setting and data**

In this section, we first overview the data annotation workflow for image recognition. We then introduce our two datasets that have been annotated via Quality Match.

### 3.1. The data annotation pipeline

A standard data annotation pipeline begins by defining the ML task and the characteristics of the data necessary to train an ML model. This ontology establishes clear guidelines for labeling and ensuring consistency across annotators. For example to train an ML model that can detect different types of obstacles observed from an onboard car camera, we may define the characteristics of pedestrians (i.e., humans with both feet on the ground) to distinguish them from motorcyclists (i.e., humans with both feet on a two-wheeled vehicle). A series of multiple choice questions (e.g., “Is the object in the image a pedestrian? Answer yes/no/can’t solve”) are constructed based on these guidelines. Each question is posed to the images or even cropped segments of images. We refer to an annotation *task* as the tuple of an image crop and a single corresponding question.

Tasks are organized and distributed to a pool of annotators through an online task assignment system. At Quality Match, this assignment system consists of a dynamic queue updated daily with the current tasks that must be completed. Annotators have the freedom to choose their own hours of employment, meaning that at any time, there may be a random pool of annotators who are servicing the queue. The assignment of a task to an annotator is referred to as a task instance or a *repeat*, and is determined randomly. Each annotator must undergo training and calibration with trial tasks to familiarize themselves with the guidelines. Moreover, annotators execute these tasks via an online interface that provides instructions and supporting labeling tools such as zooming in on an image.

Each annotation task is repeated multiple times to obtain a set of responses. Quality Match employs a majority vote to aggregate these responses and obtain the consensus ground truth response. We interchange the terms ‘response’—which refers to the multiple choice answer to the task—and ‘label’—which refers to the object in an image crop as determined by one or more annotation tasks. There may be repeats where the annotator submitted a response that differed from the majority vote. We refer to such instances as *minority reports*, i.e., disagreements with the ground truth majority.

A core challenge in this pipeline is determining how many repeats should be collected for each annotation task, since each repeat adds to the queue. A naive approach is to set a fixed number of repeats for each task, which effectively multiplies the queue length. Quality Match employs an internal dynamic protocol that estimates for each annotation task, the sample size needed for a statistically significant determination of the majority

vote (Klugmann et al. 2024). Nonetheless, this determination presents significant redundancy. Effectively, the repeats which yielded minority reports can be viewed as unnecessary instances on the annotation queue. The goal of our work is to determine just before the time of service in this queue, whether the task instance is unnecessary and can be pruned.

We may also consider variations of this data annotation pipeline or different ML tasks. For instance, tasks may be assigned via optimization to workers based on estimated worker performance. Moreover, label aggregation may involve sophisticated weighing mechanisms. Our work is agnostic to different assignment or aggregation mechanisms and lies in between these two stages, thereby allowing easy extension to alternate settings.

### 3.2. Datasets

We use two benchmark image recognition datasets, the EuroCity Persons Dataset (ECPD) (Braun et al. 2019) and the Zenseact Open Dataset (ZOD) (Alibeigi et al. 2023), as a study setting for annotator performance. ECPD is a public-access dataset containing recorded videos from the perspective of a front camera on-board vehicles driving in urban traffic environments in 12 European countries. ZOD is a public-access dataset that contains simultaneous recorded videos of multiple cameras arranged above vehicles driving around 14 European countries.

Both datasets are annotated for object detection tasks. First, the video recordings in each dataset are split into images (also referred to as frames). There are 47,000 images in ECPD and over 100,000 images in ZOD. For each image, different objects of interest are annotated via bounding boxes (also referred to as crops) that describe the coordinates of a box around each object in the image. ECPD contains bounding boxes for humans, separated into pedestrians and riders (e.g., on motorbikes, bicycles, wheelchairs). ZOD includes bounding boxes for several classes including automobiles, bicycles, wheelchairs, pedestrians, and animals. Figure 2 shows an example of an annotated frame from ECPD. Table 1 summarizes the key statistics for both datasets.

The original annotator votes for these datasets are not publicly available. Consequently for each dataset, we introduce new tasks and use the annotation service from Quality Match to re-annotate these datasets. We focus on the problem of crops containing vulnerable road users, i.e. pedestrians, cyclists, and motorcyclists, which are an important category of objects that must be detected by autonomous vehicle software. For each crop, we pose different questions which annotators can answer with ‘yes’, ‘no’, or ‘can’t solve’.

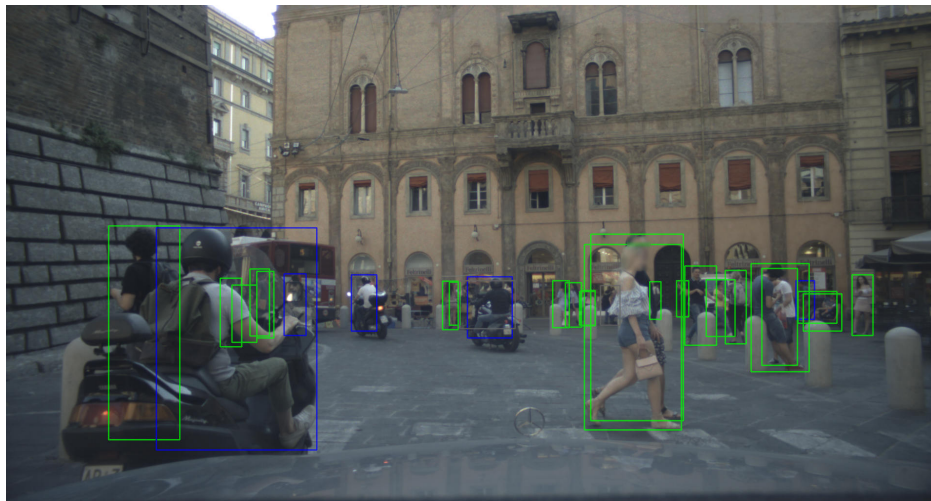


**Figure 2** A frame from ECPD with annotated bounding boxes. The green boxes correspond to crops for pedestrians and the blue boxes to crops for motorcycle riders.

	ECPD	ZOD
Observation period	Jan. 18-23, 2023	Jul. 16-17, 2024
Annotators	94	18
Images	21,776	8,488
Crops	32,741	16,000
Tasks per crop	6	1
Repeats per task	5-12	11
Total repeats	1,035,840	167,876
Frequency of responses (%)		
<i>Yes</i>	18.5	94.1
<i>No</i>	80.2	1.32
<i>Can't solve</i>	1.32	4.59
Average time spent on task (sec)	0.91	1.11
Average disagreement rate (%)	4.17	5.17

**Table 1** Summary statistics of the annotation datasets before pre-processing.

Then, over a study period of multiple days, we observe a randomly chosen cohort of annotators using the Quality Match service, to whom these tasks are assigned. Annotators choose their own hours of employment, are given detailed annotation guidelines to follow, and complete a series of tasks as determined by the daily queue. Every task is assigned to multiple annotators by Quality Match’s internal dynamic protocol. Finally, at the end of the study period, we aggregate all instances and determine the ground truth responses for each task via majority vote. We then label each instance as an agreement with the majority if the response for the instance matches the majority vote, and a minority report if the response is different from the majority vote, or a ‘can’t solve’.

On ECPD, we first select a random subset of 21,776 images from the dataset, containing a total of 32,741 crops. For every crop, we pose the following six questions:

- Q1) Is the object in the crop a human being?
- Q2) Is the object in the crop on a bicycle?
- Q3) Is the object in the crop on a poster?
- Q4) Is the object in the crop on wheels?
- Q5) Is the object in the crop a reflection from a window or mirror?
- Q6) Is the object in the crop a statue or mannequin?

We assign annotation tasks to a randomly chosen cohort of 94 annotators over a study period from January 18 to January 23, 2003, obtaining a total of 1,035,840 task instances. Each task is annotated by between five to twelve annotators. The variance in the number of repeats per task reflects the inherent ‘difficulty’ of some tasks as estimated by Quality Match’s internal assignment protocol. Figure 3a plots the number of tasks completed by annotators over the study period. We note that six workers had completed less than 100 tasks; we remove the repeats corresponding to these non-representative workers. After removing these repeats, 48 tasks had less than five repeats, making it difficult to determine an accurate ground truth via majority vote; consequently, we removed these tasks entirely from the dataset. After pre-processing, our dataset contains a total of 1,035,491 responses.

On ZOD, we first select a random subset of 8,488 images from the dataset. We then focus on only crops containing pedestrians and bicyclists within these images and ignore all other objects. For every crop, we pose the single question: Is the object in the crop a pedestrian? Consequently, an annotation task on ZOD is defined by only the crop. We assign these tasks to a randomly chosen cohort of 18 annotators over a two-day study period starting July 16, 2024. Contrasting the previous study where the number of repeats was determined via Quality Match’s internal tool, every task on ZOD is annotated by a fixed number of 11 annotators. This design ensures that our analysis is robust to different task assignment protocols. Figure 3b plots the number of tasks completed by each annotator over this study period.

We use both datasets to explore the effect of factors affecting the likelihood of a minority report. First, some objects that are in the distance, partially occluded, or blurry, can be visually hard to distinguish with respect to questions (see Figure 2). Figure 4 visualizes the histogram of the crop disagreement rate, i.e., proportion of minority reports over

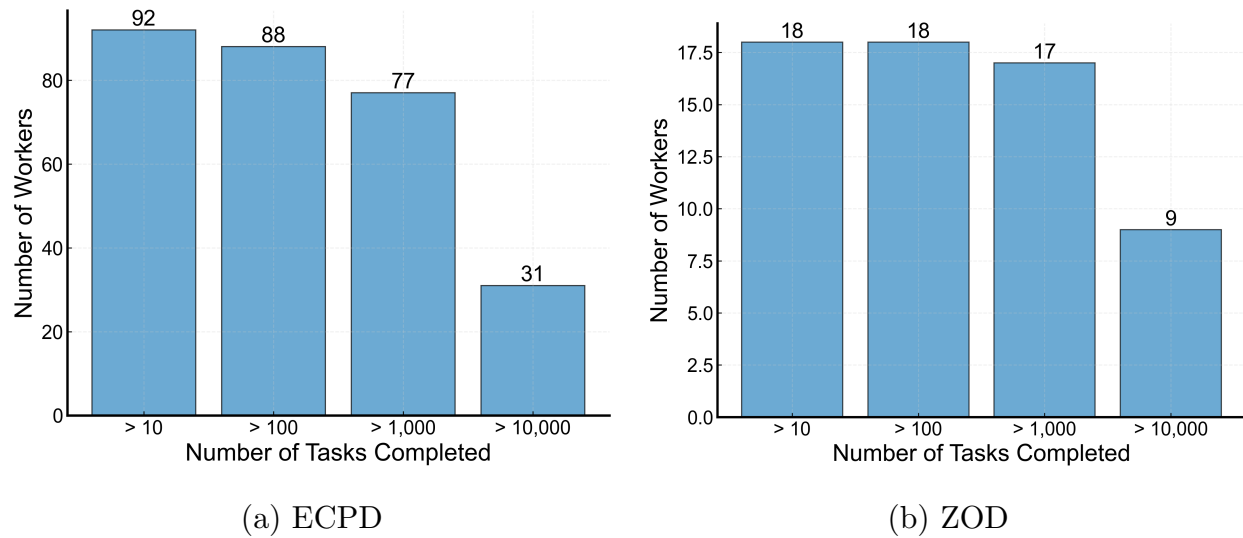


**Figure 3** The number of tasks completed by each annotator for the two datasets.

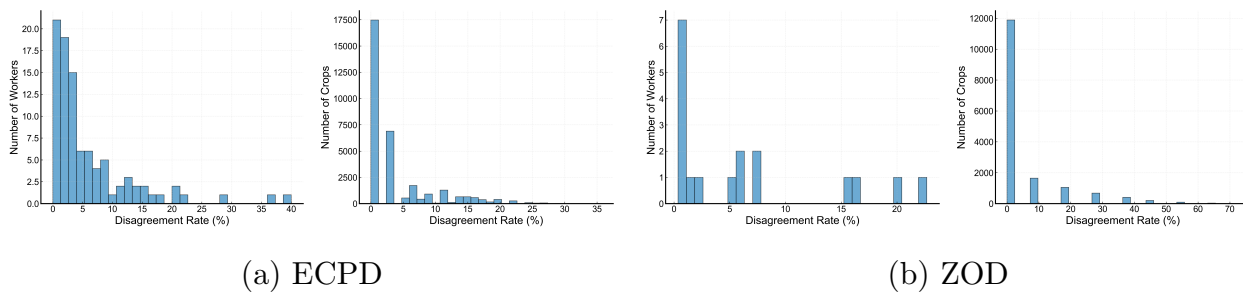


**Figure 4** For both annotation datasets: (Left) the histogram of disagreement rates per worker; (Right) the histogram of disagreement rates per crop.

all repeats in each crop. We observe Geometric distributions for both datasets. Second, crowd-sourced workers have variable skill levels for data annotation (Raykar et al. 2010, Karger et al. 2014). Figure 4 visualizes the histogram of the worker disagreement rate, i.e., proportion of minority reports produced by each worker. As with crops, we observe Geometric distributions. Finally, workers are subject to an exhaustion effect where their abilities to correctly answer questions varies as a function of how long they have been working without any rest. Figure 5 visualizes the average disagreement rate per hour aggregated over all workers on a given hour during both the ECPD and ZOD studies. We observe that the hourly disagreement rates follow a bathtub curve (O’Connor and Kleyner 2011). Intuitively, workers at the start of their day experience a warm-up period where they may be prone to making more minority reports, before achieving a steady state, until finally increasing again near the end of the shift.

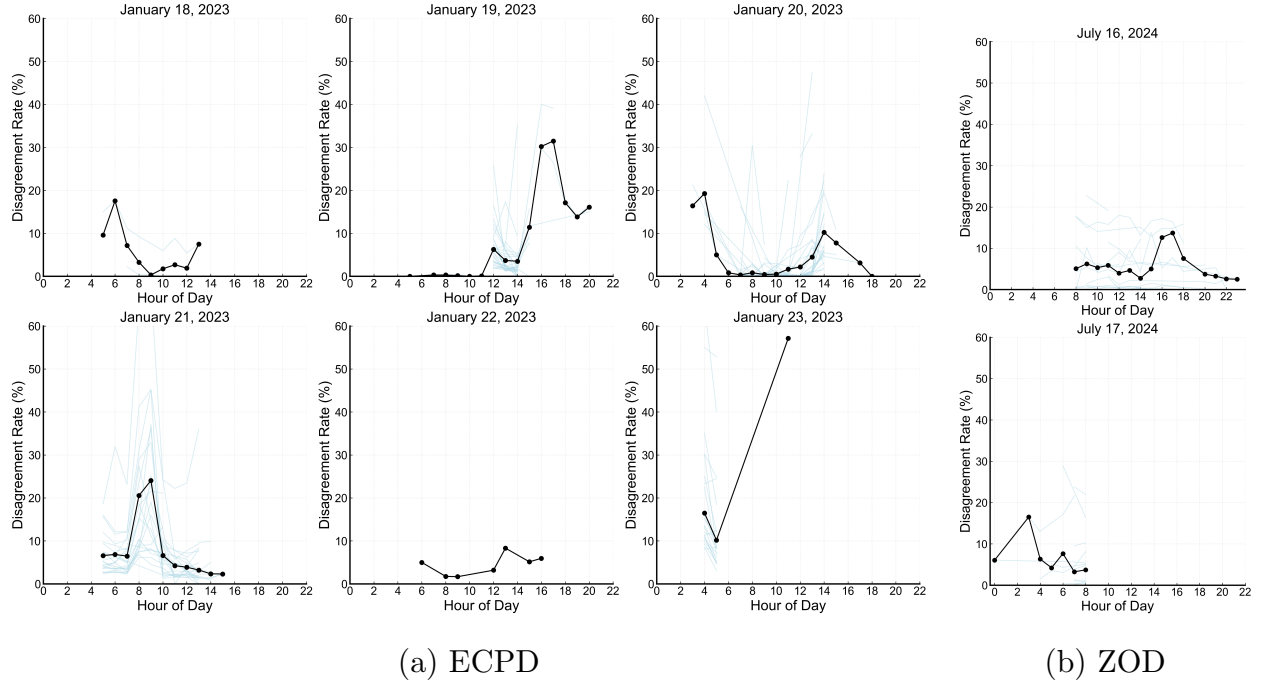


**Figure 5** The hourly disagreement rate on each day of the study. The solid black lines reflect the average disagreement rate over all active workers during that hour and the light blue lines reflect the disagreement rates for individual workers.

## 4. Empirical analysis

We empirically analyze ECPD and ZOD to model, given an annotation task assigned to a worker, the likelihood of the response being a minority report. We first formulate our logistic regression model, which captures the effect of crop and worker variability as well as worker exhaustion. We then demonstrate the effectiveness of our model and validate the importance of these covariates.

### 4.1. Model

Consider a set of image crops indexed by  $i \in \{1, 2, \dots, I\}$  where  $I$  is the total number of image crops to annotate, and a set of annotators indexed by  $j \in \{1, 2, \dots, J\}$  where  $J$  is the total number of annotators in the labor pool. Finally, suppose that for each image crop, we must annotate  $K$  different questions, indexed by  $k$ . Given an annotation task  $(i, k)$  completed by worker  $j$ , let  $y_{i,j,k} \in \{0, 1\}$  be a binary response where  $y_{i,j,k} = 1$  denotes a minority report where the worker response is either a ‘can’t solve’ or the opposite response to the majority vote. Moreover, let  $p_{i,j,k}$  denote the fitted logistic probability of the response

being a minority report. Consider the following logistic regression model:

$$\text{logit}(p_{i,j,k}) = u_i + v_j + t_{i,j,k}\beta_{t,1} + t_{i,j,k}^2\beta_{t,2} + \boldsymbol{\lambda}^\top \mathbf{x}_{i,j,k} + \epsilon_{i,j,k} \quad (1)$$

where  $u_i$  and  $v_j$  refer to latent random effect variables corresponding to the relative ambiguity in image crop  $i$  and the relative skill level of worker  $j$ , respectively. Furthermore,  $t_{i,j,k}$  refers to the amount of time (in hours) that the annotator has been continuously active on the annotation platform, while  $\beta_{t,1}$  and  $\beta_{t,2}$  are variables to capture the bathtub effect of worker activity. Given that the average time to completion of a task on ECPD is 0.91 seconds, we define a continuous period of activity as a period where the time to completion of any task has not exceeded 10 minutes. In the Online Appendix EC.1, we explore the sensitivity of our model to different definitions of continuous activity. Finally,  $\boldsymbol{\lambda}^\top \mathbf{x}_{i,j,k}$  describes the effect of control variables and  $\epsilon_{i,j,k}$  represents unobserved error. All models control for the type of question being asked (i.e., of the six questions in ECPD, some may be more challenging than others), as well as the day-of-experiment.

Conditioned on an aggregated label for a crop, the likelihood of a specific task instance being in the minority is not i.i.d. with respect to the other repeats for the same task. Furthermore, repeats may exhibit additional temporal dependency. We do not model either of these conditions due to our downstream goal of pruning annotation task assignments ex ante, when we would not have this auxiliary ground truth information. Consequently, we treat minority report events as i.i.d., but we discuss residual diagnostics in the Online Appendix EC.2.

## 4.2. Results

Table 2 summarizes the parameter estimates and goodness-of-fit of model (1) on ECPD, while Table 3 summarizes the results on ZOD. For comparison, we develop five variants: (i) *Base* containing only the control variables  $\mathbf{x}_{i,j,k}$ ; (ii) *Activity (A)* containing the control and the continuous activity variables  $t_{i,j,k}$ ; (iii) *Activity + Worker (A + W)* which include worker random effects  $v_j$ ; (iv) *Activity + Crop (A + C)* which include crop random effects  $u_i$ ; and (v) *Activity + Worker + Crop (A + W + C)* which include both worker and crop random effects. We report McFadden’s Pseudo- $R^2$  for all models by comparing against a null model with no fixed or random effects. Furthermore, Figure 7 visualizes ROC curves for each model over the two datasets. In the Online Appendix EC.2, we include additional results on our final Model A + W + C, including residual diagnostics.

	Base	A	A + W	A + C	A + W + C
Continuous activity	—	0.399*** (0.020)	0.446*** (0.022)	0.491*** (0.022)	0.542*** (0.022)
Continuous activity <sup>2</sup>	—	1.428*** (0.007)	1.306*** (0.008)	1.319*** (0.008)	1.212*** (0.008)
Crop effect $u_i$ (SD)	—	—	—	1.258	1.261
Worker effect $v_j$ (SD)	—	—	1.228	—	1.204
Human being	13.415*** (0.034)	11.401*** (0.034)	11.318*** (0.037)	13.742*** (0.035)	13.892*** (0.035)
On bike	27.515*** (0.045)	21.807*** (0.045)	26.420*** (0.063)	12.706*** (0.047)	16.353*** (0.065)
On wheels	4.966*** (0.037)	4.389*** (0.037)	3.336*** (0.041)	6.057*** (0.039)	4.679*** (0.040)
Poster	0.638*** (0.043)	0.577*** (0.043)	0.440*** (0.045)	0.590*** (0.043)	0.458*** (0.041)
Statue/mannequin	2.978*** (0.031)	2.824*** (0.032)	1.598*** (0.037)	2.828*** (0.032)	1.523*** (0.035)
Jan 18	0.569*** (0.065)	0.604*** (0.066)	1.198 (0.196)	1.541*** (0.070)	4.933*** (0.183)
Jan 19	0.069*** (0.052)	0.091*** (0.052)	0.037*** (0.072)	0.381*** (0.057)	0.152*** (0.076)
Jan 20	0.310*** (0.035)	0.334*** (0.036)	0.244*** (0.041)	0.838*** (0.039)	0.628*** (0.043)
Jan 21	0.302*** (0.027)	0.344*** (0.028)	0.200*** (0.032)	0.674*** (0.031)	0.394*** (0.034)
Jan 22	0.312*** (0.058)	0.347*** (0.058)	0.126*** (0.134)	0.470*** (0.061)	0.239*** (0.126)
Observations	1,035,491	1,035,491	1,035,491	1,035,491	1,035,491
Pseudo- $R^2$	0.0906	0.0968	0.1667	0.1527	0.2203

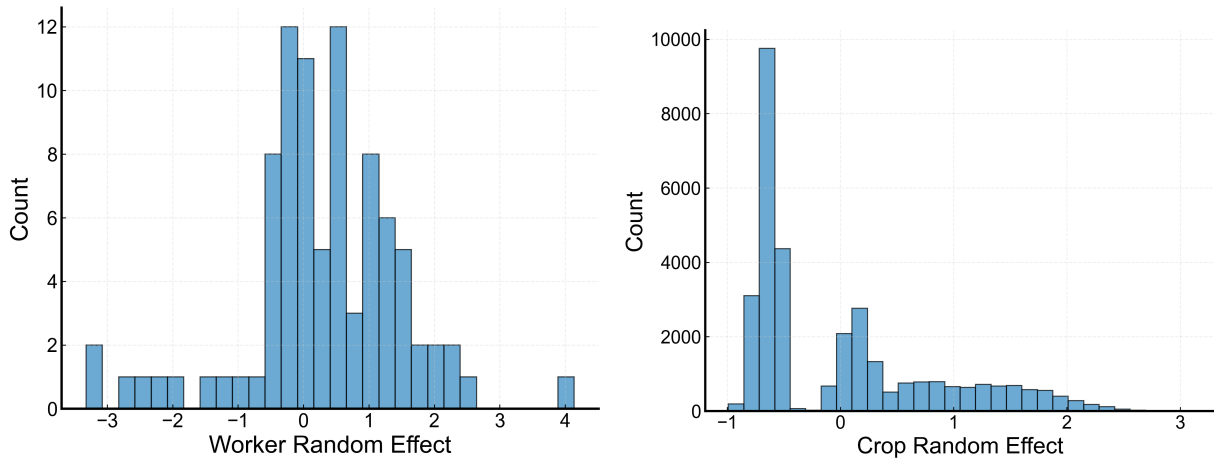
**Table 2** Comparison of odds ratios for models on ECPD. Standard errors for the log-odds are show in parentheses. For random effects, we report the standard deviation (SD) over log odds-ratios. Significance levels:

\*\*\*  $p < 0.001$ , \*\*  $p < 0.01$ , \*  $p < 0.05$ .

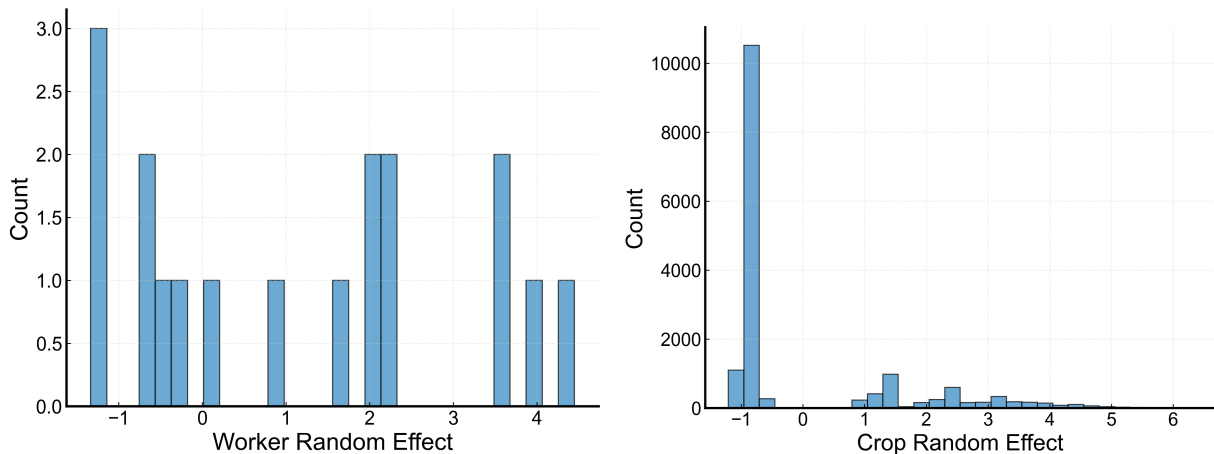
	Base	A	A + W	A + C	A + W + C
Continuous activity <sup>2</sup>	—	1.103*** (0.019)	1.016 (0.019)	1.149*** (0.023)	1.011 (0.022)
Continuous activity	—	1.023 (0.047)	0.963 (0.050)	1.022 (0.055)	0.981 (0.056)
Crop effect $u_i$ (SD)	—	—	—	2.456	2.540
Worker effect $v_j$ (SD)	—	—	1.493	—	1.640
Jul 16	1.144*** (0.025)	1.074** (0.026)	1.034 (0.032)	1.085** (0.029)	1.093* (0.036)
Observations	175,962	175,962	175,962	175,962	175,962
Pseudo- $R^2$	0.0004	0.0034	0.1589	0.1375	0.3188

**Table 3** Comparison of odds ratios for models on ZOD. Standard errors for the log-odds are show in parentheses. For random effects, we report the standard deviation (SD) over log odds-ratios. Significance levels:

\*\*\*  $p < 0.001$ , \*\*  $p < 0.01$ , \*  $p < 0.05$ .



(a) ECPD



(b) ZOD

**Figure 6** For both annotation datasets: (Left) the histogram of worker effects  $v_j$ ; (Right) the histogram of crop effects  $u_i$ . These effects represent the log-odds of a minority report given a respective worker or crop.

We first discuss the key insights drawn from the ECPD study, before discussing the ZOD study. For ECPD, the continuous activity variables are always statistically significant ( $p < 0.001$ ) when included. Furthermore, the odds ratio of the squared term is always greater than 1, which confirms the bathtub effect where the odds of a worker disagreeing on a given task is concave and decreases over time to a minimum point after which it then increases. In Figure 7a, Model A has a higher Area-Under-Curve (AUC) above the Base model by 0.1. Finally, we compare Model A with the Base model by a Likelihood Ratio Test (LRT) to confirm that this model presents a statistically significant improvement over the baseline ( $p < 0.001$ ).

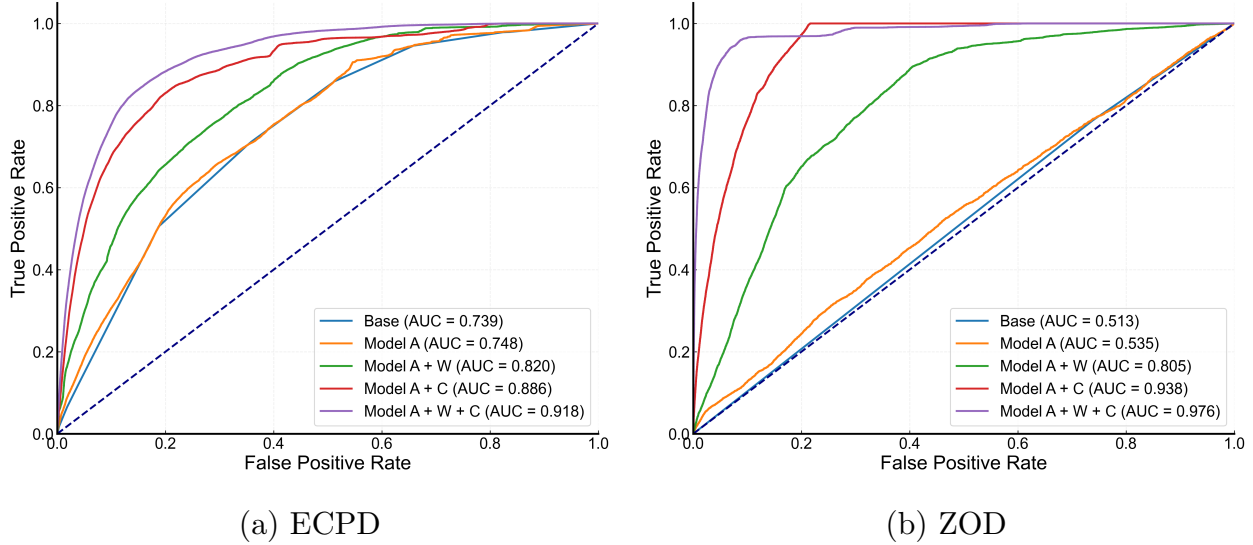


**Figure 7** ROC curves of model accuracy over both datasets. We analyze ROC in-sample to ensure all models are evaluated on the same dataset and have access to worker and crop random effects.

Incorporating worker-level (A + W) and crop-level (A + C) random effects improves upon Model A. The Pseudo- $R^2$  of these two models is larger than then Pseudo- $R^2$  of Model A by  $1.72\times$  and  $1.58\times$ . LRTs against Model A show that both Model A + W and Model A + C give statistically significant improvements over Model A ( $p < 0.001$ ). Finally, Figure 7a compares the ROC curves of these models to show that both of these models individually improve the AUC by 0.072 and 0.138 respectively. Interestingly, crop-level effects improve the predictability of disagreements by a larger margin than worker-level effects.

Finally, we combine both random effects in Model A + W + C. This model maintains similar fixed effect odds ratios and standard deviations on the random effects, while raising the Pseudo- $R^2$  over Model A + W and Model A + C by  $1.32\times$  and  $1.44\times$ , respectively. LRTs confirm that Model A + W + C improves over both Model A + W and Model A + C ( $p < 0.001$ ). Most importantly from Figure 7a, this complete model achieves an AUC of 0.918. Figure 6a also plots the histogram of both sets of random effects for Model A + W + C. There exists a long right tail over crop random effects, suggesting that while most crops have comparable levels of difficulty, there are certain crops that are significantly more difficult to annotate than the others. In the tail, the odds of some crops yielding minority reports is  $e^3 \approx 20\times$  higher. On the other hand, the worker random effect distribution is relatively symmetric, revealing a small set of highly-skilled annotators that offset the

majority of the annotators which are more error-prone. The worst-performing annotators have  $e^4 \approx 54\times$  higher odds of producing minority reports.

We now discuss the results on ZOD. First, incorporating continuous activity variables improves upon the Base model ( $p < 0.001$ ). The squared continuous activity term consistently has an odds ratio greater than 1; this verifies the bathtub curve effect observed on ECPD. However, only the squared term is statistically significant for Model A and A + C. Furthermore, incorporating both worker-level random effects (A + W) and crop-level random effects (A + C) improve upon Model A ( $p < 0.001$ ), the Pseudo- $R^2$ , and the AUC (see Figure 7b). Finally, we fit the combined Model A + W + C, which significantly improves upon all previous models ( $p < 0.001$ ), Pseudo- $R^2$ , and AUC. Figure 6b plots the histogram of random effects for Model A + W + C. Here, the crop random effect variables replicate the histogram found in ECPD. In contrast, the worker random effect distribution is more uniform than in ECPD, which is likely due to the significantly fewer number of workers used for this study.

Both datasets confirm the three factors contributing to the likelihood of disagreements. First, crop-level variability can significantly affect disagreements. While most crops are relatively unambiguous and easy-to-annotate, there are a small subset of crops with very high levels of ambiguity. Furthermore, worker-level variability affects the predictability of disagreement events by a larger degree than crop-level variability. These two trends suggest that disagreements of annotators on certain tasks can be largely predicted by estimating crop ambiguity and worker skill levels. Finally, workers experience exhaustion according a bathtub reliability curve where the start-of and end-of a continuous period of activity are more likely to yield disagreeing annotations.

## 5. Reducing repeats by pruning minority reports

We now leverage our predictive framework to proactively prune task assignments. Given a fixed set of task assignments over any given period, we estimate the likelihood of each assignment to yield a minority report, and then preemptively remove high-risk events from the annotation queue before they are assigned. Over 22% of annotation repeats can be pruned while ensuring over 99% of the task-level majority votes remain unchanged from their counterfactual ground truths. More aggressive pruning can remove over 60% of the repeats while preserving over 96% of the task-level majority votes. Interestingly, we reveal

**Algorithm 1** Iterative Pruning of Minority Reports

---

```

1: Input: Set of assigned tasks  $\mathcal{I}_t := \{(i, j, k)\}_t$  per each time period  $t \in [T]$ 
2: Initialize: Initial observation period  $\tau < T$ , classification threshold  $\theta \in [0, 1)$ , Observed annotations  $\mathcal{D} = \emptyset$ , Classification model  $p(\cdot)$ 
3: for  $t \in \{1, \dots, \tau\}$  do
4:   Observe all annotations and update  $\mathcal{D} \leftarrow \mathcal{D} \cup \mathcal{I}_t$ 
5: end for
6: Compute minority reports for all observed annotations in  $\mathcal{D}$  and fit model  $p(\cdot)$ 
7: for  $t \in \{\tau + 1, \dots, T\}$  do
8:   for Each assigned task  $(i, j, k) \in \mathcal{I}_t$  do
9:     if If task instance  $(i, k)$  and worker  $j$  are not observed in  $\mathcal{D}$  then
10:      if  $p(i, j, k) > \theta$  then
11:        Prune assignment  $\mathcal{I}_t \leftarrow \mathcal{I}_t \setminus \{(i, j, k)\}$ 
12:      end if
13:    end if
14:  end for
15:  Observe all remaining annotations and update  $\mathcal{D} \leftarrow \mathcal{D} \cup \mathcal{I}_t$ 
16:  Update minority reports for all observed annotations in  $\mathcal{D}$  and re-fit model  $p(\cdot)$ 
17: end for
18: Output: Compute majority votes for all observed annotations in  $\mathcal{D}$ 

```

---

a simple decision rule which involves pruning all repeats of annotations (i.e., setting the classification probability threshold to zero), can achieve nearly the same results as our predictive approach, highlighting significant inherent redundancy in task assignments. Finally, we ablate the importance of historical annotator data by showing that unnecessarily aggressive pruning of workers without estimating their skill effects can lead to a notable decline of around 2% in dataset quality.

### 5.1. Simulation protocol

We simulate over ECPD, which covers a large number of tasks and annotators spanned over multiple days. Algorithm 1 summarizes the steps. Our simulation emulates the annotation workflow of Quality Match and begins when a new dataset arrives and annotation tasks corresponding to image crops and questions are defined. Annotators dynamically join the pool and are allocated tasks without explicit control over these assignments.

We partition the total annotation period into  $T$  discrete intervals of fixed length  $\Delta$ , representing the frequency at which we recalibrate an estimator of the likelihood of a

minority report. For each interval  $t$ , let  $\mathcal{I}_t := \{(i, j, k)\}$  be the set of assigned tasks. During a warm-up period spanning the first  $\tau < T$  intervals, we collect and observe all completed annotations without applying any pruning. Let  $\mathcal{D} = \cup_{t \leq \tau} \mathcal{I}_t$  denote the set of all completed tasks at the end of this period. At the end of the observation phase, we determine the majority vote for each task instance  $(i, k)$  in  $\mathcal{D}$  and identify minority reports from the accumulated annotations. This historical data set is then used to fit a logistic regression model  $p(i, j, k)$  that captures the likelihood of a minority report.

At the start of each subsequent time interval  $t > \tau$ , we analyze all task assignments for the interval based on the predictive model. For each tuple  $(i, j, k)$  scheduled in the interval, we apply the following decision rule:

1. If the worker  $j$  has not been observed in  $\mathcal{D}$ , retain the assignment without pruning.
2. If the task  $(i, k)$  has not been observed in  $\mathcal{D}$ , retain the assignment without pruning.
3. Otherwise, estimate the probability  $p(i, j, k)$  of this assignment being a minority report. If  $p(i, j, k) > \theta$  for a fixed threshold  $\theta \in [0, 1)$ , then prune the task from  $\mathcal{I}_t$ .

At the end of interval  $t$ , we then update our observed dataset of completed tasks  $\mathcal{D}$  with  $\mathcal{I}_t$ . We then use the updated  $\mathcal{D}$  to recalibrate the logistic regression model for the next interval. In our experiments, we establish  $\tau = 36$  hours (i.e., Jan. 18 12:00AM to Jan. 19 12:00PM) and recalibrate the model every  $\Delta = 1$  hour. We further evaluate intervals of  $\Delta = 2, 4, 8, 24, \infty$  hours, where the final setting refers to no recalibration.

Our predictive model is a class-balanced mixed effects logistic regression using only worker and crop random effects and the question type. This model and our decision rule are designed for simplicity and flexibility. While we may consider alternative predictive models or sophisticated strategies, the proposed setup requires no additional data beyond the specific worker-task assignment. Moreover, the recalibration step requires less than two minutes of computational time on a standard MacBook M1 Pro laptop with 32 GB RAM. Finally, our framework permits additional constraints depending on annotation platform requirements (e.g., we may consider at least three repeats per annotation task to ensure a robust majority vote).

We benchmark our pruning strategy against two baselines. The first baseline, *No Predictions (NP)*, employs a simple decision rule without any predictions where we prune all repeated assignments observed, i.e., pruning with a threshold  $\theta = 0$ . Interestingly, this naive strategy achieves nearly competitive performance to our predictive approach at aggressive

	Experiment	Accuracy	$F_1$ score	Prune rate (%)
Ours ( $\Delta = 1$ hr.)	$\theta = 0.99$	99.1	0.985	22.4
	$\theta = 0.93$	97.5	0.956	39.5
	$\theta = 0.1$	96.4	0.933	60.9
NP	$\Delta = 1$ hr.	96.5	0.933	68.7
	$\Delta = 2$ hr.	96.7	0.937	52.0
	$\Delta = 4$ hr.	97.6	0.952	37.1
	$\Delta = 8$ hr.	97.8	0.955	33.2
	$\Delta = \infty$	99.3	0.986	11.7

**Table 4** Dataset quality measured by accuracy and  $F_1$  score versus the prune rate on ECPD for different strategies. NP refers to the No Pruning baseline.

pruning thresholds. The second baseline, *All workers (AW)* relaxes the condition requiring prior worker observation (i.e., step 1 in the decision rule). This allows us to prune decisions even for newly observed workers by assigning zero random effects.

We evaluate all strategies along three metrics. We first track the Prune Rate, which quantifies the fraction of task repeats (out of 1,035,491) that were pruned from the queue. We then measure the final dataset quality in terms of the majority votes of each task instance post-simulated pruning versus the ground truth majority vote of the counterfactual where no repeats are pruned. Here, we use  $F_1$  score and Accuracy with respect to the yes/no labels. The  $F_1$  score addresses dataset imbalance as most task instances have ground truth response ‘no’.

## 5.2. Tradeoffs between cost and dataset quality

Table 4 highlights the metrics for our pruning strategy. First, employing our predictive model with hourly recalibration ( $\Delta = 1$  hour) and a high pruning threshold ( $\theta = 0.99$ ) enables us to eliminate 22.4% of the annotation repeats while maintaining an  $F_1$  score of 0.985. Here, over 99% of the 196,446 annotation tasks have the same majority vote as the counterfactual ground truth. Given that annotation instances take on average 0.91 seconds, this pruning translates to an estimated 2.4 days across the annotation period or approximately 36 minutes saved per annotator on average. Lowering the pruning threshold to  $\theta = 0.93$  can remove 39.5% of repeats, while maintaining an  $F_1$  score of 0.956 or 97.5% accuracy. This translates to removing an estimated 4.3 days or approximately 1.1 hours saved per annotator. Finally, an aggressive threshold  $\theta = 0.1$  can prune 60.9% of the repeats, while maintaining an  $F_1$  score of 0.933 and 96.4% accuracy. This translates to 6.6 days equivalent or approximately 1.7 hours per annotator over the study period saved.

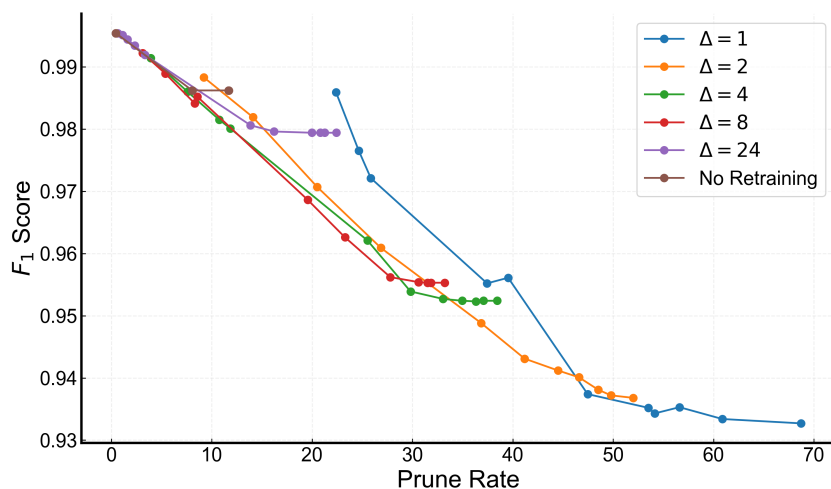


**Figure 8** Evaluating the effect of different re-training frequencies ( $\Delta$ ). The rightmost point on each curve represents the NP baseline.

There is an inherent tradeoff where pruning tasks can reduce the annotation time, and therefore, costs, but at the risk of lowering annotation quality. Benchmark ML datasets range between 1% to 10% in terms of the fraction of erroneous labels (Northcutt et al. 2021). Even in our most aggressive pruning setting, our framework achieves an error rate of 4.6%, while the more conservative pruning strategies yield error rates of 2.5% and 0.9%.

Different downstream ML tasks require different levels of quality. For instance, the error tolerance on computer vision for classifying pedestrians near a vehicle may be lower compared to consumer video conferencing applications such as detecting people in front of a web camera. An annotation team may select  $\theta$  appropriately depending on the application to yield the corresponding appropriate reduction in annotation cost at the expense of some acceptable loss in dataset quality.

### 5.3. Importance of selective pruning via decision rules

We next ablate the effectiveness of our strategy via the recalibration frequency and by relaxing the pruning criteria. Figure 8 visualizes the tradeoff between the prune rate and the  $F_1$  score at different  $\Delta$  frequencies of recalibration. More frequent recalibration allows the observed dataset  $\mathcal{D}$  to be up-to-date with information about annotators and crops that have just recently entered the work pool and queue, respectively. Recalibration every 1 to 2 hours achieves Pareto-optimal performance while less frequent recalibration results in substantially lower prune rates for the same level of dataset quality. For example, recalibrating every 24 hours can at best yield a prune rate of 22% at  $F_1$  score of 0.979, which is

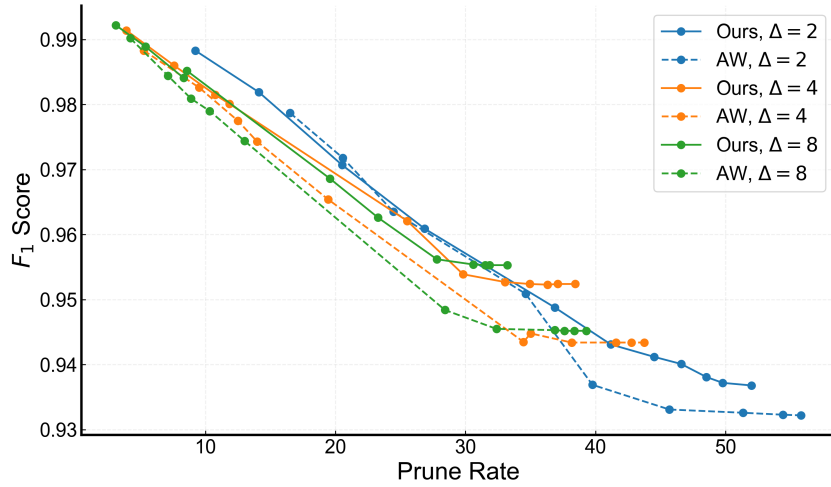


**Figure 9** Ablating the loss in dataset quality when pruning via the AW strategy, which relaxes the first decision criteria.

lower than the conservative pruning strategy ( $\theta = 0.1$ ) for  $\Delta = 1$ . Moreover, the remaining 78% of the annotation repeats do not qualify for the first two decision rules. We similarly observe that recalibrating at  $\Delta = 4$  and  $\Delta = 8$  can prune at best 37% and 33% of the annotation repeats, respectively.

We next directly ablate the effectiveness of the decision rules against a baseline strategy (AW) which relaxes the first decision rule of pruning only workers that have been seen in the observational dataset. Here, the regression model cannot factor the new worker’s latent skill effect. Figure 9 compares our strategy against AW for  $\Delta = 2, 4, 8$ . In each case, the ablation strategy results in a noticeable drop in downstream  $F_1$  score for a given prune rate.

#### 5.4. Surprising effectiveness of always pruning

Finally, we benchmark our strategy against a simple model-free baseline, NP, that consistently prunes all observed repeat tasks that pass the first two decision rules. This is equivalent to setting  $\theta = 0$  and can be observed by the rightmost point for each curve in Figure 8. This policy uses a single parameter  $\Delta$  to control how often to recalibrate the memory of observed tasks, making this a simple decision rule-based framework to implement. Table 4 highlights the performance of this approach for different values of  $\Delta$ . For any fixed level of retraining, NP is competitive with the most aggressive pruning setting of our predictive approach. Moreover, this policy appears on the Pareto frontier when considered against slower recalibration frequencies, i.e.,  $\Delta > 2$ . Unfortunately, NP does not

provide significant user control in balancing the cost-dataset quality tradeoff, as it can only achieve certain discrete points on the curve. Notably for downstream applications that require high levels of dataset quality, our predictive strategy with regular recalibration (i.e.,  $\Delta = 1$ ) consistently dominates the simple baseline. We conclude that while the current annotation practice enforces a high degree of redundancy that can be reduced with simple heuristics, pruning by estimating the likelihood of a minority report can yield a noticeable improvement and permit more precise positioning within the cost-quality tradeoff.

## 6. The theoretic cost-accuracy tradeoff

In this section, we theoretically analyze a stylized model of repeated annotation tasks to better understand the observed tradeoff between pruning costs and the resulting dataset accuracy. We define the overall dataset accuracy as a function of a given classification model and probability of a minority report and prove that removing annotation repeats always increases the risk of reversing the aggregated majority vote. This reveals a ‘no free lunch’ principle within pruning for data annotation. Moreover, we simulate the accuracy measure to yield rule-of-thumb guidelines for the number of repeats and the type of classifier to use in pruning-based annotator management. We leave all proofs to the Online Appendix EC.3.

Our theoretical framework relies on the following assumptions.

*ASSUMPTION 1. Each annotation task is repeated by  $n$  workers who can only make binary yes/no votes, where  $n$  is an odd number. The unconditional ex ante probability of a worker disagreeing with the majority vote is  $p$ .*

We view  $p$  as the average disagreement rate of a dataset, for example, with  $p = 0.0417$  for ECPD. Our ex ante probability assumption differs slightly from the classical crowd-sourced task aggregation literature, which assumes that each annotation task has an unknown ground truth label and that instances identify the correct label with i.i.d. probability (Dawid and Skene 1979, Raykar et al. 2010, Karger et al. 2014). This difference is due to the fact that the ground truth in our setting (i.e., as prescribed by Quality Match) is defined by the counterfactual majority vote of  $n$  workers. Furthermore, although Assumption 1 enforces a fixed number of repeats, our analysis naturally generalizes to variable repeat counts by conditioning on each potential value of  $n$ .

ASSUMPTION 2. *We have access to a binary classifier to predict a minority report, parametrized by a true positive rate  $q_T$  and false positive rate  $q_F \leq q_T$ .*

Assumption 2 characterizes the classifier by true positive and false positive rates. In practice, these parameters are induced by the threshold  $\theta$  of a logistic regression model.

### 6.1. The value of pruning and aggregating votes

For notation, let  $\bar{p} := 1 - p$ ,  $\bar{q}_T := 1 - q_T$ , and  $\bar{q}_F := 1 - q_F$ . The probability of flipping the aggregated majority vote can be computed by counting the number of incorrectly pruned majority votes and the number of true minority votes that remain.

THEOREM 1. *Suppose Assumptions 1 and 2 hold. Without loss of generality, assume errors in tie events. Then, the probability of an incorrectly annotated object after pruning is  $P_{err} := (S(p, q_T, q_F) + T(p, q_T, q_F))/C(p)$  where*

$$\begin{aligned} S(p, q_T, q_F) &:= \sum_{k=\lfloor \frac{n}{2} \rfloor + 1}^{n-1} \sum_{i=0}^{n-k-1} \sum_{j=2k-n+i}^k \binom{n}{k} \binom{n-k}{i} \binom{k}{j} \bar{p}^k p^{n-k} q_T^i \bar{q}_T^{n-k-i} q_F^j \bar{q}_F^{k-j} \\ T(p, q_T, q_F) &:= \sum_{k=\lfloor \frac{n}{2} \rfloor + 1}^n \binom{n}{k} \bar{p}^k p^{n-k} q_T^{n-k} q_F^k \\ C(p) &:= \sum_{k=\lfloor \frac{n}{2} \rfloor + 1}^n \binom{n}{k} \bar{p}^k p^{n-k}. \end{aligned}$$

From Theorem 1, we can estimate the accuracy of the annotated dataset after pruning as  $1 - P_{err}$ . We may bound how many tasks to remove before the accuracy degrades below an acceptable level.

Figure 10 plots the dataset accuracy as a function of  $p$  under several different classifiers. We note that aggregating a large number of annotations and pruning the ones estimated to be redundant is typically more accurate than simply aggregating a fewer number of annotations. Specifically, a classifier with  $(q_T = 0.5, q_F = 0.5)$  (i.e., red curve) is equivalent to aggregating only a random 50% of the annotations. For example with  $n = 11$ , this curve approximates the counterfactual where we only obtain on average 5.5 annotations per task. This red curve is almost always worse than the other annotation curves. However for sufficiently small  $p$  and high  $n$ , pruning annotations with a poor classifier is less effective than simply performing fewer annotations.

While accuracy decreases with increasing  $p$ , the rate of decrease varies significantly depending on  $q_T$  and  $q_F$ . Even if  $p = 0$ , aggressive classifiers with high  $q_F$  can ruin the

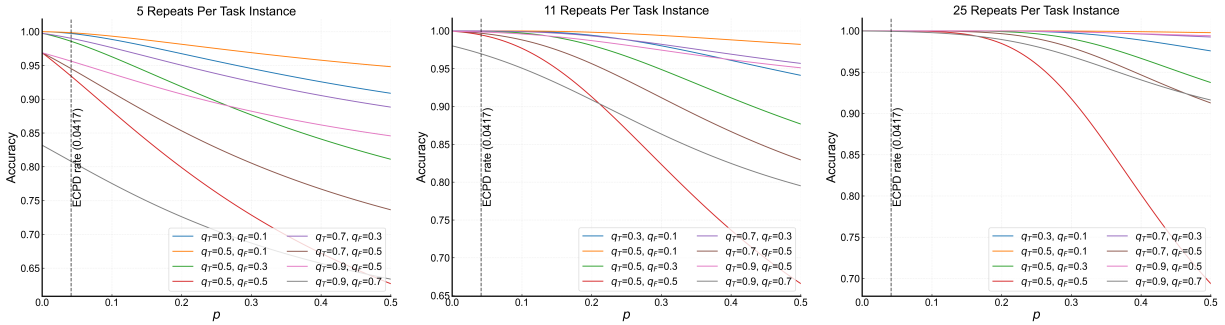


**Figure 10** Dataset annotation accuracy as a function of the individual annotator minority report rate  $p$  when annotation repeats are pruned with different ML models defined by  $(q_T, q_F)$ . The red curve represents  $(q_T = 0.5, q_F = 0.5)$ , i.e., a random classifier that prunes 50% of the annotations. The plots consider  $n = 5, 11, 25$  repeats.

dataset by incorrectly predicting assignments as minority reports. In practice and in Section 4, we mitigate this issue via a decision rule that each annotation task must have at least one completed task assignment. Furthermore, aggressive models with higher  $q_T$  and  $q_F$  are more effective when  $p$  is sufficiently large. For instance when  $n = 5$  and  $p > 0.3$ , the model with  $(q_T = 0.9, q_F = 0.5)$  is better than the model with  $(q_T = 0.5, q_F = 0.3)$ .

Finally, we observe the impact of the number of repeats needed for a high-quality dataset. Specifically at the ECPD disagreement rate, with  $n = 11$  or with  $n = 5$  and a classifier with sufficiently low  $q_F$ , the overall dataset accuracy is consistently above 95%; this reflects our empirical observations in Section 4. This analysis further allows us to obtain rule-of-thumb estimates for how many repeats are recommended based on the average rate of annotator disagreement. For instance, we observe that our framework can consistently ensure above 95% accuracy even for all  $p < 0.1$ .

## 6.2. The cost-accuracy tradeoff

To analyze the relationship between the amount of data pruned and the overall dataset quality, we first confirm that holding the classifier fixed, a larger  $p$  decreases the expected accuracy of the pruned dataset.

**THEOREM 2.** *If Assumptions 1 and 2 hold,  $P_{err}$  monotonically increases with  $p$ .*

While we have explored the relationship between worker behavior and the accuracy of the downstream dataset, we next connect this relationship to the prune rate, i.e., the fraction of repeats being pruned from the dataset. Given  $p$ , as well as a true positive rate  $q_T$  and false positive rate  $q_F$ , the prune rate is  $r := pq_T + \bar{p}q_F$ . From Assumption 2,  $q_T > q_F$ ,

which means that  $r$  is a non-decreasing function of  $p$  for a fixed model. Consequently,  $P_{err}$  must also increase with  $r$ .

**COROLLARY 1.** *Suppose Assumptions 1 and 2 hold. For a fixed classifier,  $P_{err}$  monotonically increases with  $r$ .*

Theorem 2 and Corollary 1 imply a ‘no free lunch’ property where pruning annotations will always reduce dataset accuracy at the benefit of reducing the annotation cost, measured by number of annotations. Intuitively, none of the repeats are ‘strictly redundant’ ex ante and have some probability of altering the aggregated label. If we accept a modest 5% error rate, then we can prune a large proportion of the task assignments. Example 1 below showcases this property.

**EXAMPLE 1.** *Consider a logistic regression classifier defined by model parameters  $\boldsymbol{\lambda}$  and threshold  $\theta$  where  $1/(1 + \exp(-\mathbf{x}_{i,j,k}^\top \boldsymbol{\lambda})) > \theta$  implies that the task assignment  $(i, j, k)$  is predicted to be a minority report. Suppose  $\mathbf{x}_{i,j,k}^\top \boldsymbol{\lambda} | y_{i,j,k} = 1 \sim \mathcal{N}(\mu_1, \sigma^2)$  and  $\mathbf{x}_{i,j,k}^\top \boldsymbol{\lambda} | y_{i,j,k} = 0 \sim \mathcal{N}(\mu_0, \sigma^2)$  where  $\mu_1 > \mu_0$  and  $\sigma > 0$  are Gaussian parameters. Then, the true positive rate and false positive rate are*

$$q_T(\theta) = \Pr \left\{ \mathbf{x}_{i,j,k}^\top \boldsymbol{\lambda} > \text{logit}(\theta) \mid y_{i,j,k} = 1 \right\} = 1 - F_1(\text{logit}(\theta))$$

$$q_F(\theta) = \Pr \left\{ \mathbf{x}_{i,j,k}^\top \boldsymbol{\lambda} > \text{logit}(\theta) \mid y_{i,j,k} = 0 \right\} = 1 - F_0(\text{logit}(\theta))$$

where  $F_1(\cdot)$  and  $F_0(\cdot)$  are the CDF of  $\mathcal{N}(\mu_1, \sigma)$  and  $\mathcal{N}(\mu_0, \sigma)$ , respectively. Furthermore,  $r(p, \theta) = p(1 - F_1(\text{logit}(\theta))) + \bar{p}(1 - F_0(\text{logit}(\theta)))$ .

Figure 11 plots the accuracy as a function of  $r(p, \theta)$  for different values of  $p$ , after setting  $\mu_1 = 0.5, \mu_0 = -0.5, \sigma = 1$ . For this classifier, the AUC = 0.760. Note that this choice of parameters implies significant overlap between the two covariate distributions. Nonetheless, the plots reveal significant redundancy where even for  $n = 5$ , up to  $r = 50\%$  of the repeats can be pruned while preserving approximately 95% accuracy. For  $n = 11$  and  $n = 25$ , we can prune over 70% and 85% of the annotation repeats, respectively, at the same level of accuracy. These plots reflect the observations from our empirical analysis where we were able to prune 68.7% of the repeats while preserving over 95% accuracy in the final dataset.

## 7. Conclusion and discussion

In this paper, we investigate how existing data annotation pipelines for ML systems can be further optimized to reduce labor costs while preserving data quality. We introduce the

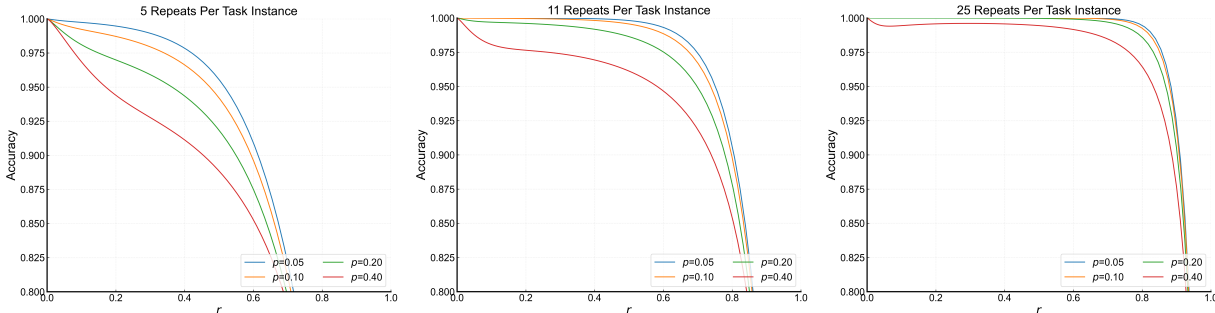


**Figure 11** From Example 1, annotation accuracy as a function of the prune rate  $r$ .; We set  $\mathbf{x}_{i,j,k}^\top \boldsymbol{\lambda} | y_{i,j,k} = 1 \sim \mathcal{N}(0.5, 1)$  and  $\mathbf{x}_{i,j,k}^\top \boldsymbol{\lambda} | y_{i,j,k} = 0 \sim \mathcal{N}(-0.5, 1)$ , meaning the AUC = 0.760. The three plots consider settings where each task instance has 5, 11, and 25 repeats, respectively.

notion of minority reports, referring to annotator responses that deviate from the final crowd consensus label. By predicting the likelihood of an assigned annotation task being a minority report using worker- and task-specific covariates, our framework effectively prunes costly task assignments before they occur. We validate this approach through extensive empirical analysis in collaboration with Quality Match, a high-quality data annotation firm, on two object detection datasets that were annotated under the firm’s operational procedures. Our findings show that pruning can reduce the annotation volume by over 60% at only a small sacrifice in dataset accuracy that is consistent with the standard error levels in most benchmark datasets (Northcutt et al. 2021).

The data annotation pipeline is a complex process involving collecting data, proposing a labeling ontology, crafting annotation tasks, assigning these tasks to a worker pool, and then aggregating their responses. Our pruning treatment easily fits into existing data annotation pipelines, since pruning operates in the layer after tasks are assigned but before they are executed. Below, we highlight several insights for data annotation platforms and suggestions for future work.

**Balancing cost versus quality for downstream tasks.** Our method identifies and dynamically removes task assignments for which annotators are likely to produce erroneous response, thereby reducing labeling costs for a given acceptable data quality level. Safety-critical ML applications such as in medical imaging or autonomous vehicles can adopt conservative thresholds, while applications with higher degrees of acceptable ML prediction error can aggressively prune annotation tasks to reduce costs. Moreover, we navigate this tradeoff via a single thresholding parameter. Finally, while we focus on computer vision

tasks, the paradigm of pruning minority reports easily applies to any ML setting where data is annotated via a majority vote to determine a ‘ground truth’ answer.

**Rule-of-thumb estimates on how much to annotate and prune.** Our analysis yields easily calculable estimates of dataset quality and savings from pruning as a function of the annotator disagreement rate and summary metrics of a classifier. Consequently, practitioners can easily determine appropriate pruning decision rules to achieve the desired cost-quality tradeoff without further costly experimentation in parameter tuning. In particular, we show that assigning a larger number of repeats and pruning potential minority reports will typically produce higher quality data than simply assigning fewer annotations.

**Annotator behavior and the potential for worker-personalized interventions.** Our empirical analysis reveals that the combination of crop ambiguity or difficulty, annotator skill, and annotator fatigue can accurately estimate the likelihood of an annotator producing a minority report. Although not implemented, we believe our model can drive additional operational treatments to better manage the annotator pool. For instance, annotation platforms may use the annotator effect variables to identify potential low-skilled workers and provide personalized additional calibration and retraining sessions. Platforms may also employ fatigue-aware task scheduling, for instance with scheduled breaks to mitigate these fatigue-related errors. This may also promote better working conditions and improve the overall well-being of annotators, contributing to sustainable and responsible labeling practices.

We envision expanding this framework along several directions. Firstly, it is increasingly common to merge human annotation with AI support, which can take the form of identifying high-value points that require accurate labels or by providing initial labels that human annotators can just verify rather than label themselves. Trends among worker skills and fatigue can differ in this setting as the task of verifying a label is fundamentally different from the task of creating a label. Furthermore, the emerging class of large language models warrant different annotation paradigms such as in reinforcement learning with human feedback (RLHF), where human annotators must annotate the outputs of models according to ranked preferences. The high variability in human preference prevents clear majority votes or even permits multiple different notions of a ground truth label (Liu et al. 2024). Moreover, annotation in RLHF is typically more time-consuming and considered expensive human labor, as it may require specialized expertise (Liu et al. 2025). Nonetheless,

we believe that analytics-driven task assignment and pruning rules can benefit ML teams seeking to minimize annotation costs without compromising data integrity.

## References

- Adelman D, Mersereau A, Pakiman P (2024) Dynamic assignment of jobs to workers with learning curves. *Available at SSRN 4964890* .
- Alibeigi M, Ljungbergh W, Tonderski A, Hess G, Lilja A, Lindström C, Motorniuk D, Fu J, Widahl J, Petersson C (2023) Zenseact open dataset: A large-scale and diverse multimodal dataset for autonomous driving. *Proceedings of the IEEE/CVF International Conference on Computer Vision*, 20178–20188.
- Berg J, Furrer M, Harmon E, Rani U, Silberman MS (2018) Digital labour platforms and the future of work: Towards decent work in the online world .
- Bigelow P, Brulte G (2024) Tesla’s data advantage. The Road to Autonomy, URL <https://www.roadtoautonomy.com/tesla-data-advantage/>.
- Bouajaja S, Dridi N (2017) A survey on human resource allocation problem and its applications. *Operational Research* 17:339–369.
- Braun M, Krebs S, Flohr FB, Gavrilu DM (2019) Eurocity persons: A novel benchmark for person detection in traffic scenes. *IEEE Transactions on Pattern Analysis and Machine Intelligence* 1–1, ISSN 0162-8828.
- Cai X, Gong J, Lu Y, Zhong S (2018) Recover overnight? work interruption and worker productivity. *Management Science* 64(8):3489–3500.
- Dawid AP, Skene AM (1979) Maximum likelihood estimation of observer error-rates using the em algorithm. *Journal of the Royal Statistical Society: Series C (Applied Statistics)* 28(1):20–28.
- Deng J, Dong W, Socher R, Li LJ, Li K, Fei-Fei L (2009) Imagenet: A large-scale hierarchical image database. *2009 IEEE Conference on Computer Vision and Pattern Recognition*, 248–255 (Ieee).
- Dimensional Research (2019) Artificial intelligence and machine learning projects are obstructed by data issues: Global survey of data scientists, ai experts and stakeholders. Technical report.
- Durasov N, Mahmood R, Choi J, Law MT, Lucas J, Fua P, Alvarez JM (2024) Uncertainty estimation for 3d object detection via evidential learning. *arXiv preprint arXiv:2410.23910* .
- Fatehi S, Wagner MR (2022) Crowdsourcing last-mile deliveries. *Manufacturing & Service Operations Management* 24(2):791–809.
- Goh HW, Tkachenko U, Mueller JW (2023) CROWDLAB: Supervised learning to infer consensus labels and quality scores for data with multiple annotators. *arXiv preprint arXiv:2210.06812* Workshop on Human-in-the-Loop Learning, NeurIPS 2022.
- Gonzalez-Cabello M, Siddiq A, Corbett CJ, Hu C (2024) Fairness in crowdwork: Making the human ai supply chain more humane. *Business Horizons* .

- Gurvich I, O’Leary KJ, Wang L, Van Mieghem JA (2020) Collaboration, interruptions, and changeover times: workflow model and empirical study of hospitalist charting. *Manufacturing & Service Operations Management* 22(4):754–774.
- Hanbury A (2008) A survey of methods for image annotation. *Journal of Visual Languages & Computing* 19(5):617–627.
- Hartig F (2016) Dharma: residual diagnostics for hierarchical (multi-level/mixed) regression models. *CRAN: Contributed Packages* .
- Horton JJ (2011) The condition of the turking class: Are online employers fair and honest? *Economics Letters* 111(1):10–12.
- Horton JJ, Chilton LB (2010) The labor economics of paid crowdsourcing. *Proceedings of the 11th ACM conference on Electronic Commerce*, 209–218.
- Jagabathula S, Subramanian L, Venkataraman A (2017) Identifying unreliable and adversarial workers in crowdsourced labeling tasks. *Journal of Machine Learning Research* 18(93):1–67.
- Jin Y, Duan Y, Ding Y, Nagarajan M, Hunte G (2020) The cost of task switching: Evidence from emergency departments. *Available at SSRN 3756677* .
- Karger DR, Oh S, Shah D (2014) Budget-optimal task allocation for reliable crowdsourcing systems. *Operations Research* 62(1):1–24.
- Kaynar N, Siddiq A (2023) Estimating effects of incentive contracts in online labor platforms. *Management Science* 69(4):2106–2126.
- Kc DS, Staats BR (2012) Accumulating a portfolio of experience: The effect of focal and related experience on surgeon performance. *Manufacturing & Service Operations Management* 14(4):618–633.
- Khetan A, Oh S (2016) Achieving budget-optimality with adaptive schemes in crowdsourcing. *Advances in Neural Information Processing Systems* 29.
- Kittur A, Nickerson JV, Bernstein MS, Gerber E, Shaw A, Zimmerman J, Lease M, Horton JJ (2013) The future of crowd work. *Proceedings of the 2013 Conference on Computer Supported Cooperative Work (CSCW)* (New York, NY, USA: ACM).
- Klugmann C, Mahmood R, Hegde G, Kale A, Kondermann D (2024) No need to sacrifice data quality for quantity: Crowd-informed machine annotation for cost-effective understanding of visual data. *arXiv preprint arXiv:2409.00048* .
- Lanzarone E, Matta A (2014) Robust nurse-to-patient assignment in home care services to minimize overtimes under continuity of care. *Operations Research for Health Care* 3(2):48–58.
- Liao YH, Acuna D, Mahmood R, Lucas J, Prabhu VU, Fidler S (2024) Transferring labels to solve annotation mismatches across object detection datasets. *The Twelfth International Conference on Learning Representations*.

- Liao YH, Kar A, Fidler S (2021) Towards good practices for efficiently annotating large-scale image classification datasets. *Proceedings of the IEEE/CVF Conference on Computer Vision and Pattern Recognition (CVPR)*, 4350–4359.
- Liu S, Pan Y, Chen G, Li X (2024) Reward modeling with ordinal feedback: Wisdom of the crowd. *arXiv preprint arXiv:2411.12843* .
- Liu S, Wang H, Zhongyao M, Li X (2025) How humans help llms: Assessing and incentivizing human preference annotators. *arXiv preprint arXiv:2502.06387* .
- Manshadi VH, Rodilitz S (2022) Online policies for efficient volunteer crowdsourcing. *Management Science* 68(9):6572–6590.
- Narayanan S, Balasubramanian S, Swaminathan JM (2009) A matter of balance: Specialization, task variety, and individual learning in a software maintenance environment. *Management science* 55(11):1861–1876.
- Northcutt CG, Athalye A, Mueller J (2021) Pervasive label errors in test sets destabilize machine learning benchmarks. *arXiv preprint arXiv:2103.14749* .
- O’Connor P, Kleyner A (2011) *Practical reliability engineering* (john wiley & sons).
- Palley AB, Satopää VA (2023) Boosting the wisdom of crowds within a single judgment problem: Weighted averaging based on peer predictions. *Management Science* 69(9):5128–5146.
- Raykar VC, Yu S, Zhao LH, Valadez GH, Florin C, Bogoni L, Mozer M (2010) Learning from crowds. *Journal of Machine Learning Research* 11:1297–1322.
- Rodrigues F, Pereira FC (2018) Deep learning from crowds. *Proceedings of the 32nd AAAI Conference on Artificial Intelligence (AAAI)*.
- Song H, Kim M, Park D, Shin Y, Lee JG (2022) Learning from noisy labels with deep neural networks: A survey. *IEEE transactions on neural networks and learning systems* 34(11):8135–8153.
- Staats BR, Gino F (2012) Specialization and variety in repetitive tasks: Evidence from a japanese bank. *Management science* 58(6):1141–1159.
- Stratman EG, Boutilier JJ, Albert LA (2024) Decision-aware predictive model selection for workforce allocation. *arXiv preprint arXiv:2410.07932* .
- Tan Z, Li D, Wang S, Beigi A, Jiang B, Bhattacharjee A, Karami M, Li J, Cheng L, Liu H (2024) Large language models for data annotation: A survey. *arXiv preprint arXiv:2402.13446* .
- Tanno R, Saeedi A, Sankaranarayanan S, Alexander DC, Silberman N (2019) Learning from noisy labels by regularized estimation of annotator confusion. *Proceedings of the IEEE Conference on Computer Vision and Pattern Recognition (CVPR)*, 11236–11245.
- Tian X, Shi J, Qi X (2022) Stochastic sequential allocations for creative crowdsourcing. *Production and Operations Management* 31(2):697–714.

- Vila M, Pereira J (2014) A branch-and-bound algorithm for assembly line worker assignment and balancing problems. *Computers & Operations Research* 44:105–114.
- Wang J, Ipeirotis PG, Provost F (2017) Cost-effective quality assurance in crowd labeling. *Information Systems Research* 28(1):137–158.
- Wen Z, Lin L (2016) Optimal fee structures of crowdsourcing platforms. *Decision Sciences* 47(5):820–850.
- Yin J, Luo J, Brown SA (2021) Learning from crowdsourced multi-labeling: A variational bayesian approach. *Information Systems Research* 32(3):752–773.
- Yin M, Suri S, Gray ML (2018) Running out of time: The impact and value of flexibility in on-demand crowdwork. *Proceedings of the 2018 CHI Conference on Human Factors in Computing Systems (CHI)* (New York, NY, USA: ACM).

Parameter	Default	1 minute	30 minutes	60 minutes
Continuous activity <sup>2</sup>	1.428*** (0.007)	1.345*** (0.024)	1.071*** (0.002)	1.016*** (0.001)
Continuous activity	0.399*** (0.020)	0.519*** (0.037)	0.799*** (0.011)	0.934*** (0.008)
Observations	1,035,491	1,035,491	1,035,491	1,035,491
Pseudo- $R^2$	0.0968	0.0918	0.0947	0.0915

**Table EC.1** Comparison of odds ratios for Model A with different definitions of ‘Continuous activity’ on ECPD.

The default definition is 10 minutes. Standard errors for the log-odds are show in parentheses. For random effects, we report the standard deviation (SD) over log odds-ratios. Significance levels: \*\*\*  $p < 0.001$ , \*\*  $p < 0.01$ , \*  $p < 0.05$ .

## Online Appendix for Minority Reports: Balancing Cost and Quality in Ground Truth Data Annotation

### EC.1. Robustness to continuous activity

In Section 4.2, Model A consisted of a logistic regression model to predict the odds of a minority report given the amount of continous time that the annotator had spent working. Here, continuous activity was defined as the uninterrupted period of task completion, with breaks of at least 10 minutes marking the start of a new activity period. In this section, we explore the robustness of Model A to alternative definitions of continuous activity.

To assess robustness, we re-estimate the mixed-effects logistic regression models using alternative break thresholds of one minute, 30 minutes, and 60 minutes. Table EC.1 summarizes these results, as well as the default 10 minute break version (Model A from Table 2) for reference. Across all model specifications, the coefficients for Continuous Activity and Continuous Activity<sup>2</sup> remain statistically significant ( $p < 0.001$ ), indicating robustness to the choice of threshold. The coefficient magnitudes are relatively stable. Most importantly, the squared term consistently has an odds ratio greater than one, confirming the presence of the bathtub fatigue effect. Finally, we remark that the Pseudo- $R^2$  values remain consistent.

### EC.2. Residual diagnostics

We examine the residual diagnostics associated with the final logistic regression model, i.e., Model A + W + C, developed in Section 4.2. To investigate residual variance, we conduct dispersion tests for both datasets (Hartig 2016). Results indicate no significant evidence of

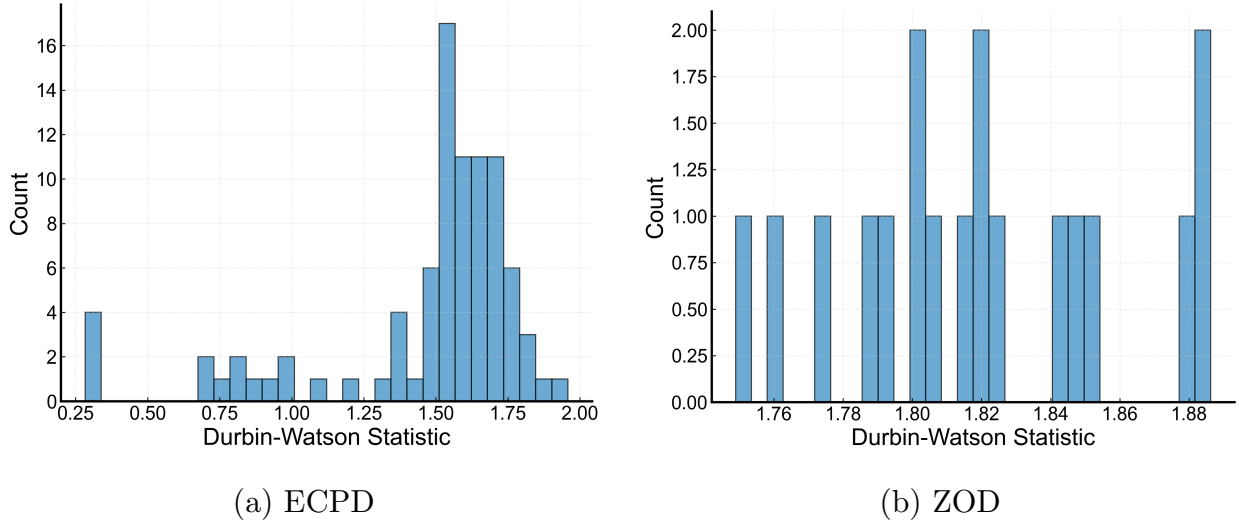


**Figure EC.1** For both annotation datasets, the histogram of Durbin-Watson statistics for each annotator over the corresponding study period.

either over-dispersion or under-dispersion in the residuals ( $p > 0.05$ ), thereby confirming homoscedasticity.

To ensure independence of the residuals with respect to autocorrelation, we compute Durbin-Watson statistics via deviance residuals for each annotator’s task throughout the study period. Figure EC.1 plots the histogram of these statistics. For both datasets, most annotators exhibit Durbin-Watson values exceeding 1.5. This indicates some minor positive autocorrelation for annotators.

### EC.3. Proofs

*Proof of Theorem 1* For any fixed  $n$  repeats, let  $K$  be a random variable representing the number of votes constituting the majority. Given that disagreements are i.i.d.,  $K$  follows a truncated Binomial distribution where

$$\Pr\{K = k\} = \frac{1}{C(p)} \binom{n}{k} \bar{p}^{n-k} p^k, \quad \forall K \geq \lfloor \frac{n}{2} \rfloor + 1$$

Given a classifier, after the repeats that are predicted to be disagreements are removed from the set of votes, the final majority vote will change if and only if the remaining count of disagreements exceeds the remaining count of the prior majority. Let  $T_{n-k} \sim \text{Binomial}(n - k, q_T)$  be a random variable representing the number of True Positive (TP) detections conditioned on  $K = k$  majority votes. Finally, let  $F_k \sim \text{Binomial}(k, q_F)$  be a

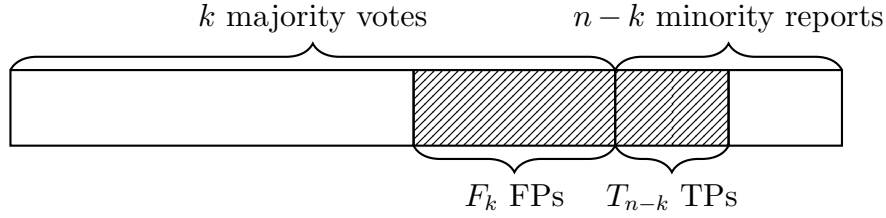


**Figure EC.2** Visualizing the false positive (FPs) and true positives (TP) predictions on an annotation task with  $n$  repeats, conditioned on  $k \leq n - 1$  initial votes for the majority. For the majority vote to change, we must have  $T_{n-k} \leq n - k - 1$  and  $F_k \geq 2k - n + T_{n-k}$ .

random variable representing the number of False Positive (FP) detections conditioned on  $K = k$  majority votes.

The majority vote may change, under two disjoint events:

i) There are  $K = k \leq n - 1$  votes towards the majority (i.e., at least one minority report). Furthermore, there are at most  $T_{n-k} \leq n - k - 1$  TPs; and  $F_k \geq 2k - n + T_{n-k}$  FPs. This ensures that the original majority votes after pruning are counted to  $k - F_k \leq n - k - T_{n-k}$  votes for the minority and that at least one vote remains. Figure EC.2 visualizes this event.

ii) All repeats are pruned, i.e.,  $F_k = k$  and  $T_{n-k} = n - k$ .

We will prove that  $S(p, q_T, q_F)/C(p)$  is equal to the likelihood of the first event, and  $T(p, q_T, q_F)/C(p)$  is equal to the likelihood of the second event.

The first event can be characterized as

$$\begin{aligned}
& \sum_{k=\lfloor \frac{n}{2} \rfloor + 1}^{n-1} \Pr\{K = k\} \Pr\{T_{n-k} \leq n - k - 1 \text{ and } F_k \geq 2k - n + T_{n-k} \mid K = k\} \\
&= \sum_{k=\lfloor \frac{n}{2} \rfloor + 1}^{n-1} \Pr\{K = k\} \sum_{i=1}^{n-k-1} \Pr\{T_{n-k} = i \mid K = k\} \sum_{j=2k-n+i}^k \Pr\{F_k = j \mid K = k\} \\
&= \frac{1}{C(p)} \sum_{k=\lfloor \frac{n}{2} \rfloor + 1}^{n-1} \sum_{i=0}^{n-k-1} \sum_{j=2k-n+i}^k \binom{n}{k} \binom{n-k}{i} \binom{k}{j} \bar{p}^k p^{n-k} q_T^i \bar{q}_T^{n-k-i} q_F^j \bar{q}_F^{k-j}
\end{aligned}$$

where the second line follows from the independence of TP and FP detections and the third line follows from the definitions of each of the probability mass functions. The last line is equal to  $S(p, q_T, q_F)/C(p)$ .

The second event is characterized as

$$\sum_{k=\lfloor \frac{n}{2} \rfloor + 1}^n \Pr\{K = k\} \Pr\{F_k = k \text{ and } T_{n-k} = n - k \mid K = k\} = \frac{1}{C(p)} \sum_{k=\lfloor \frac{n}{2} \rfloor + 1}^{n-1} \binom{n}{k} \bar{p}^k p^{n-k} q_T^{n-k} q_F^k$$

where the equality follows from the independence of  $F_k$  and  $T_{n-k}$  and their definitions as Binomial distributions. This is equal to  $T(p, q_T, q_F)/C(p)$ .

The total  $P_{err}$  is the sum of these two events, which completes the proof.

Before proving Theorem 2, we first require the following helper Lemma.

LEMMA EC.1. *Suppose Assumptions 1 and 2 hold. Let*

$$\beta_k := \Pr\{F_k \geq 2k - n + T_{n-k} \text{ and } T_{n-k} \leq n - k - 1\} \quad (\text{EC.1})$$

$$\gamma_k := \Pr\{F_k = k \text{ and } T_{n-k} = n - k\} \quad (\text{EC.2})$$

Then, both  $\beta_k$  and  $\gamma_k$  are non-increasing in  $k$ .

*Proof of Lemma EC.1* We first prove for  $\beta_k$ . Since  $F_k$  and  $T_{n-k}$  are independent Binomial distributions, we can define  $F_{k+1} = F_k + Y$  and  $T_{n-k-1} = T_{n-k} - Z$  where  $Y \sim \text{Bernoulli}(q_F)$  and  $Z \sim \text{Bernoulli}(q_T)$  are independent Bernoulli distributions. Then, we want to prove the inequality:

$$\begin{aligned} & \Pr\{F_k \geq 2k - n + T_{n-k} \text{ and } T_{n-k} \leq n - k - 1\} \\ & \geq \Pr\{F_{k+1} \geq 2(k+1) - n + T_{n-k-1} \text{ and } T_{n-k-1} \leq n - k - 2\} \\ & = \Pr\{F_k \geq 2k - n + T_{n-k} + (2 - Y - Z) \text{ and } T_{n-k} \leq n - k - 1 + (Z - 1)\} \end{aligned}$$

where the equality follows from the definition of  $F_{k+1}$  and  $T_{n-k-1}$ .

To prove the inequality, note that both  $2 - Y - Z \geq 0$  and  $Z - 1 \leq 0$  with probability 1. Therefore, the event space of both events in the right-hand-side must be a subset of the events in the left-hand-side.

We now prove for  $\gamma_k$ . Consider the ratio

$$\frac{\gamma_{k+1}}{\gamma_k} = \frac{\binom{k+1}{k+1} \binom{n-k-1}{n-k-1} q_T^{k+1} \bar{q}_T^0 q_F^{n-k-1} \bar{q}_F^0}{\binom{k}{k} \binom{n-k}{n-k} q_T^k \bar{q}_T^0 q_F^{n-k} \bar{q}_F^0} = \frac{q_F}{q_T} < 1. \quad (\text{EC.3})$$

Above, the first equality follows from the definition of the probabilities, and the second equality follows from reducing the terms. The inequality follows from Assumption 2, which states  $q_F < q_T$ . This completes the proof.

We are now ready to prove Theorem 2.

*Proof of Theorem 2* To prove that the label quality decreases with  $p$ , it suffices to show that  $P_{err}$  will increase monotonically with  $p$ . For notational simplicity, we will rewrite  $P_{err}$  below. First, let  $\hat{k} := \lfloor \frac{n}{2} \rfloor + 1$  and let  $g_k(p) := \binom{n}{k} (1-p)^k p^{n-k}$ . Then,

$$S(p) := \sum_{k=\hat{k}}^{n-1} g_k(p) \beta_k \quad T(p) := \sum_{k=\hat{k}}^n g_k(p) \gamma_k,$$

where  $\beta_k$  is defined as in (EC.1) and  $\gamma_k$  is defined as in (EC.2). Note that we will omit the dependency on  $p, q_T, q_F$  for all functions when it is obvious.

We will prove that each of the two terms of  $P_{err} = S(p)/C(p) + T(p)/C(p)$  both increase monotonically with  $p$  by showing that their derivatives with respect to  $p$  are non-negative.

We first consider  $S(p)/C(p)$ . Note that

$$\frac{d}{dp} \left( \frac{S}{C} \right) = \frac{S'C - SC'}{C^2}.$$

Since the denominator is positive for  $p \in (0, 1)$ , we must only prove that the numerator is positive. We first use the following log trick to compute the derivative of  $g_k(p)$  below:

$$\frac{d \log g_k(p)}{dp} = \frac{d \log g_k(p)}{dg_k(p)} \frac{dg_k(p)}{dp} = \frac{n-k}{p} - \frac{k}{1-p} \iff g'_k = g_k \left( \frac{n-k}{p} - \frac{k}{1-p} \right).$$

Consequently,

$$S' = \sum_{k=\hat{k}}^{n-1} g_k \left( \frac{n-k}{p} - \frac{k}{1-p} \right) \beta_k \quad C' = \sum_{m=\hat{k}}^n g_m \left( \frac{n-m}{p} - \frac{m}{1-p} \right),$$

where we use subscript  $m$  for  $C(p)$  to avoid overloading the subscript for  $S(p)$ .

Finally,

$$S'C - SC' = \left( \sum_{k=\hat{k}}^{n-1} g_k \left( \frac{n-k}{p} - \frac{k}{1-p} \right) \beta_k \right) \left( \sum_{m=\hat{k}}^n g_m \right) - \left( \sum_{k=\hat{k}}^{n-1} g_k \beta_k \right) \left( \sum_{m=\hat{k}}^n g_m \left( \frac{n-m}{p} - \frac{m}{1-p} \right) \right) \quad (\text{EC.4})$$

$$= \sum_{k=\hat{k}}^{n-1} \sum_{m=\hat{k}}^n g_k g_m \beta_k \left( \frac{n-k}{p} - \frac{k}{1-p} \right) - \sum_{k=\hat{k}}^{n-1} \sum_{m=\hat{k}}^n g_k g_m \beta_k \left( \frac{n-m}{p} - \frac{m}{1-p} \right) \quad (\text{EC.5})$$

$$= \sum_{k=\hat{k}}^{n-1} \sum_{m=\hat{k}}^n g_k g_m \beta_k \left( \frac{n-k}{p} - \frac{k}{1-p} - \frac{n-m}{p} + \frac{m}{1-p} \right) \quad (\text{EC.6})$$

$$= \frac{1}{p(1-p)} \sum_{k=\hat{k}}^{n-1} \sum_{m=\hat{k}}^n g_k g_m \beta_k (m-k) \quad (\text{EC.7})$$

Above, (EC.5) follows from expanding the sum products, (EC.6) follows from grouping the two summations together, and (EC.7) follows from factoring the denominators.

Note that the summands will be positive for all  $m > k$ , negative for  $m < k$ , and zero otherwise. We use this to decompose the summation and apply a symmetry argument below:

$$\text{RHS (EC.7)} = \frac{1}{p(1-p)} \left( \sum_{k=\hat{k}}^{n-1} \sum_{m=\hat{k}}^{k-1} g_k g_m \beta_k (m-k) + \sum_{k=\hat{k}}^{n-1} \sum_{m=k+1}^n g_k g_m \beta_k (m-k) \right) \quad (\text{EC.8})$$

$$= \frac{1}{p(1-p)} \left( \sum_{m=\hat{k}}^n \sum_{k=m+1}^{n-1} g_k g_m \beta_k (m-k) + \sum_{k=\hat{k}}^{n-1} \sum_{m=k+1}^n g_k g_m \beta_k (m-k) \right) \quad (\text{EC.9})$$

$$= \frac{1}{p(1-p)} \left( \sum_{k=\hat{k}}^n \sum_{m=k+1}^{n-1} g_m g_k \beta_m (k-m) + \sum_{k=\hat{k}}^{n-1} \sum_{m=k+1}^n g_k g_m \beta_k (m-k) \right) \quad (\text{EC.10})$$

$$= \frac{1}{p(1-p)} \left( \sum_{k=\hat{k}}^{n-1} \sum_{m=k+1}^n g_k g_m \beta_k (m-k) - \sum_{k=\hat{k}}^n \sum_{m=k+1}^{n-1} g_m g_k \beta_m (m-k) \right) \quad (\text{EC.11})$$

$$= \frac{1}{p(1-p)} \left( \sum_{k=\hat{k}}^{n-1} \sum_{m=k+1}^{n-1} g_k g_m (\beta_k - \beta_m) (m-k) + \sum_{k=\hat{k}}^{n-1} g_n g_k \beta_k (n-k) \right) \quad (\text{EC.12})$$

Above, (EC.8) decomposes the sum into two components over  $m < k$  and  $m > k$ , respectively. Then, (EC.9) reorders the sums inside the first component and (EC.10) applies a change of variables  $m \rightarrow k, k \rightarrow m$ . Then, (EC.11) reorders the two components.. Finally, (EC.12) combines the two components into one large sum and a remainder component.

Finally, note that in RHS (EC.12), each of the summands inside both components are positive, since  $g_k, g_m > 0$  always,  $\beta_k \geq \beta_m > 0$  for all  $m > k$  due to Lemma EC.1, and  $m-k > 0, n-k > 0$  inside their sums. Consequently,  $S'C - SC' \geq 0$ , meaning that  $S(p)/C(p)$  has a non-negative derivative and increases monotonically with  $p$ .

We now prove for  $T(p)/C(p)$  using a similar argument. Note that

$$\frac{d}{dp} \left( \frac{T}{C} \right) = \frac{T'C - TC'}{C^2},$$

meaning we only need to show that  $T'C - TC' > 0$ , where  $T' = \sum_{k=\hat{k}}^n g_k ((n-k)/p - k/(1-p)) \gamma_k$  can be determined with the same steps as before for  $S'$  and  $C'$ . Next,

$$T'C - TC' = \left( \sum_{k=\hat{k}}^n g_k \left( \frac{n-k}{p} - \frac{k}{1-p} \right) \gamma_k \right) \left( \sum_{m=\hat{k}}^n g_m \right) - \left( \sum_{k=\hat{k}}^n g_k \gamma_k \right) \left( \sum_{m=\hat{k}}^n g_m \left( \frac{n-m}{p} - \frac{m}{1-p} \right) \right) \quad (\text{EC.13})$$

$$= \frac{1}{p(1-p)} \sum_{k=\hat{k}}^n \sum_{m=k+1}^n g_k g_m (\gamma_k - \gamma_m)(m-k). \quad (\text{EC.14})$$

We arrive at (EC.14) by following the same steps in (EC.5)–(EC.12). Next, note that  $\gamma_k - \gamma_m > 0$  from Lemma EC.1 and that  $m - k > 0$ . Therefore,  $T'C - TC' > 0$ , meaning that  $T(p)/C(p)$  has a non-negative derivative and increases monotonically with  $p$ . This completes the proof.

*Proof of Corollary 1* First, note that  $r(p)$  is invertible and differentiable in  $p$ . Let  $\rho(r) = p$  denote the inverse function of  $r(p)$  and consider  $(S(p) + T(p))/C(p) = (S(\rho(r)) + T(\rho(r)))/C(\rho(r))$ . We prove below that the derivative of this function is positive for all  $r$ . First, by the chain rule:

$$\frac{d}{dr} \left( \frac{S(\rho(r))T(\rho(r))}{C(\rho(r))} \right) = \frac{d}{d\rho} \left( \frac{S(\rho) + T(\rho(r))}{C(\rho)} \right) \frac{d\rho}{dr}. \quad (\text{EC.15})$$

From Theorem 2, the first term in the product is positive for all  $\rho$ . Furthermore, from the inverse function theorem,

$$\frac{d\rho}{dr} = \frac{1}{\frac{d}{dp}r(\rho(r))} > 0 \quad (\text{EC.16})$$

where the inequality comes from the observation that  $dr/dp > 0$  for all  $p$ . Therefore, the product in (EC.15) is the product of a positive and a positive number, meaning that it is also positive.